RESEARCH MONOGRAPH NO. 9

Corrosion of steel in reinforced concrete: Influence of binder type, water/binder ratio, cover and cracking

M.G. ALEXANDER
H. BEUSHAUSEN
M.B. OTIENO

Collaborative research by the
University of Cape Town and the
University of the Witwatersrand

INDUSTRY/NRF COLLABORATIVE RESEARCH PROGRAMME: ACHIEVING DURABLE AND ECONOMIC CONCRETE CONSTRUCTION IN THE SOUTH AFRICAN CONTEXT

SERIES OF RESEARCH MONOGRAPHS

The work reported in this monograph, and others in the series, has arisen from a research programme into how to achieve durable and economic concrete construction in the South African context. The present programme has been in existence since 1997, and is a joint collaborative effort between research students and staff at the University of Cape Town and the University of the Witwatersrand. The monographs are essentially compilations of theses, research papers and reports that have emanated from the programme, and consequently the work of the research students is acknowledged.

This particular monograph represents work done by A. Scott and M. Otieno towards their PhD and MSc (Eng) degrees respectively, at the University of Cape Town. The authors wish to acknowledge with gratitude the following for financial support of this work:
• Cement and Concrete Institute (C&CI)
• National Research Foundation (NRF)
• Sika (SA) Pty Ltd
• Concrete Manufacturers' Association
• Tertiary Education Support Programme (TESP) of Eskom
• Water Research Commision (WRC)

M.G. Alexander, H. Beushausen, M.B. Otieno;
September 2012

See inside back cover for a list of monographs in this series

RESEARCH MONOGRAPH NO. 9

Corrosion of steel in reinforced concrete:

Influence of binder type, water/binder ratio, cover and cracking

M G Alexander
H Beushausen
M B Otieno

Concrete Materials and Structural Integrity Research Unit
Department of Civil Engineering
University of Cape Town

Published by the Concrete Materials and Structural Integrity Research Unit,
Department of Civil Engineering, University of Cape Town

2012

Layout by Mike Otieno

Printed by Fingerprint, Epping

Contents

Acknowledgements

The authors would like to acknowledge the research contribution by Dr Allan Scott during his doctoral work at the University of Cape Town. We also express our appreciation for research funding from the South African cement and concrete industries via the Cement and Concrete Institute, and from the National Research Foundation. Specifically, we would like to thank Pretoria Portland Cement Ltd (PPC), Afrisam South Africa (Pty) Ltd and Sika South Africa (Pty) Ltd for their valuable support.

This monograph has been published with the financial support of Pretoria Portland Cement Ltd (PPC), for which we express thanks.

Foreword

The concrete materials research programme at UCT and Wits has done extensive work on durability of concrete in the last two decades. Much of this work has focused on the transport properties of concrete, and on devising practical, scientifically sound approaches to controlling and specifying concrete durability in new construction. This has resulted in the Durability Index Approach, which is now being implemented in major projects nationally (Ballim, 1993, Alexander *et al*. 2001, Mackechnie and Alexander, 2001). Several earlier monographs in this series were based on this and other work (a full list of the monographs can be found on the inside back cover of this monograph). However, the focus has now been extended to corrosion control and prediction, and how to manage deteriorating infrastructure so as to extract maximum life and economic value from it. This monograph represents this extension of research focus.

In contrast to most of the previously published monographs in this series, Monograph 9 does not focus mainly on providing practical guidelines for practising engineers, although the information will of course be useful. Rather, it aims at the education of postgraduate students, academics and structural engineers interested in the field of reinforcement corrosion. Much useful work has been done with respect to identifying the mechanisms of steel reinforcement corrosion in concrete. However, for practical guidelines on how to include reinforcement corrosion modelling in service life design of concrete structures, further research is necessary. This monograph summarizes our existing knowledge on reinforcement corrosion in concrete, expands on research done at the University of Cape Town, and highlights the need for future research.

(Note that the terms ‘cement’ and ‘binder’ are used interchangeably in this monograph.)

INTRODUCTION

This monograph is concerned with steel corrosion in reinforced concrete (RC) structures. This is a difficult and pervasive problem worldwide for concrete engineers and practitioners. Premature deterioration due to reinforcing steel corrosion now represents one of the most serious threats to the future of concrete as the foremost construction material for infrastructure (Figure 1). Consequently, it has received much research attention. Unfortunately little of this research has found expression in practice. The aim of this monograph is to help practising engineers understand the issues so as to be able to design and construct reinforced concrete structures better.

Figure 1: Corrosion-induced damage on a concrete bridge exposed to air-borne chlorides close to the shore in Cape Town

The following should be noted:

1. In most urbanising regions worldwide, a vast amount of infrastructure needs to be put in place in coming decades, consuming large quantities of concrete.
2. Compared to previous practice, owners and managers of concrete infrastructure will require far greater assurance of a maintenance-free service life of their assets.

3. The changing environment, including the effects of climate change, are likely to pose greater risks to concrete durability than previously experienced.
4. A large stock of existing concrete infrastructure has reached the end of its design and economic life, but cannot be replaced and needs life extension strategies to be applied.
5. In many countries, the amount spent on repair and rehabilitation of existing concrete infrastructure by far exceeds the amount spent for new construction.
6. Concrete binder systems are becoming increasingly sophisticated and complex, for which no long-term performance data are available.
7. There is growing pressure for sustainable construction, including greater resource conservation and increased use of alternative materials such as recycled materials.

In view of these issues, it is clear that engineers will need to design more durable structures, as well as manage deteriorating ones better.

In recent decades, good understanding on transport mechanisms in uncracked concrete has been developed. However, reinforced concrete structures are designed to crack in service. Concrete is an inherently cracked material. Cracking originates from a variety of causes and at all stages during the service life of a concrete structure. At early ages, microcracking is induced by the differential thermal and shrinkage properties of hydrates and aggregates. Cracking can also be induced by plastic shrinkage or settlement prior to setting of the concrete. Poor curing and thermal gradients can lead to additional surface cracking during the first few days after casting. At later stages, load and shrinkage induced stresses may cause major cracking. Additional cracking can arise from environmental effects, and occasionally due to internal chemical incompatibility, e.g. Alkali-Aggregate Reaction (AAR). Importantly, cracking has a critical influence on the performance and life of the structure. It is only relatively recently that attention has been focused on corrosion studies in cracked reinforced concrete. It is important to understand the influence of cracking on corrosion of the embedded steel, and the resulting consequences for the service life of the structure.

The monograph is based partly on the thesis work of Scott (Scott, 2004) and Otieno (Otieno, 2008). They both investigated corrosion of reinforcing steel in cracked and uncracked reinforced concrete. Scott studied a series of cement blends incorporating blast furnace slag, fly ash and silica fume. As part of his work, he studied pore solution chemistry of the

different cement blends and corrosion kinetics of steel in simulated pore solutions. Otieno also studied corrosion in blended cements, but these were restricted to Corex slag blends. His main focus was the influence of crack widths on corrosion rate, and the influence of Corex slag blends on corrosion of steel in cracked reinforced concrete.

Some background is needed in understanding the behaviour of these systems, including a basic understanding of the characteristics and mechanisms of steel corrosion in reinforced concrete and the influence of cement blends. Consequently, the monograph covers the fundamentals of steel corrosion, followed by pertinent results from the work of Scott and Otieno: aqueous phase studies of simulated pore solutions and steel corrosion in these solutions, and the influence of crack width on steel corrosion in blended cement concretes, respectively. The influence of steel cover is also dealt with. The results are generalised into a framework for understanding steel corrosion that should assist design engineers in their task.

Scott and Otieno worked with different slags. Scott used ground granulated blastfurnace slag (from Gauteng), while Otieno used Corex slag (from the Western Cape). While these slags are different, particularly in their physical characteristics and their effect on concrete strength, they have similar effects in respect of concrete durability in chloride exposures - which is the main environment covered in this monograph. Thus, their results can be viewed as a whole and generalised into useful insights.

The monograph is divided into two Parts:

- Part I is an introduction to the fundamentals of steel corrosion in reinforced concrete as a necessary background to understanding the work reported in the second part.
- Part II is a résumé of the experimental corrosion studies carried out at UCT on steel in simulated pore solutions (in order to highlight the relevant chemical factors), and on cracked and uncracked reinforced concrete specimens.

An Appendix gives salient details of the experimental work, including the materials, concrete mixtures, and testing.

PART I: CORROSION OF STEEL IN CONCRETE – BACKGROUND

FUNDAMENTALS OF STEEL CORROSION IN CONCRETE

This section deals with fundamental issues relating to reinforcement corrosion in concrete, including corrosion mechanisms, damage modelling, measurement techniques, and the influence of cracks.

a) Three-stage corrosion damage model

Reinforcement corrosion in concrete is linked mainly to carbonation of the concrete or chloride penetration into the concrete. Both of these cause the steel to become thermodynamically unstable (i.e. de-passivated - see later) and therefore liable to corrode. Once the steel starts to corrode actively, it results in degradation of the concrete structure and may threaten its structural performance.

The deterioration of RC structures due to steel corrosion involves three stages as shown in Figure 2 (Heckroodt, 2002):

(i) An initiation period before corrosion begins, during which little or no damage occurs. However, during this period, the ingress of harmful substances such as chlorides and carbon dioxide takes place which can eventually result in de-passivation of the steel reinforcement and consequently cause reinforcement corrosion. The ingress of harmful substances and the progress of carbonation are largely controlled by concrete quality (penetrability), pore solution chemistry, environmental exposure conditions, cover depth, and possible cracking of the concrete.

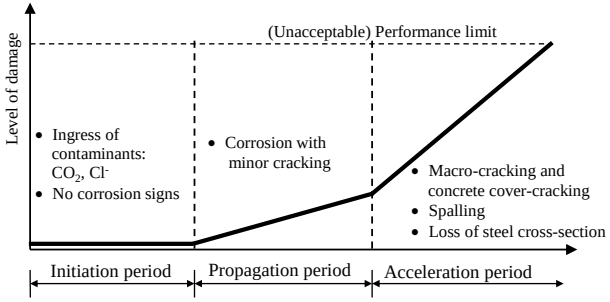

Figure 2: Three-stage corrosion damage model (Heckroodt, 2002)

(ii) A propagation phase after corrosion activation that generates expansive corrosion products, causing cracking of the cover concrete.
(iii) An acceleration phase where corrosion rate increases due to easy access of oxygen, moisture and aggressive agents through cracks and spalls. Damage is clearly visible, there is loss of steel cross-section, and the concrete cover may be of little value in controlling corrosion due to extensive cracking and spalling.

b) Corrosion cells

Corrosion of reinforcing steel in concrete is an electrochemical process, whereby a corrosion cell is set up in which two types of electrodes are formed, namely anodes and cathodes. The electrochemical process involves the flow of ions and electrons resulting from chemical interactions between a thermodynamically unstable metal and an electrolyte. This flow results in an electrical current between an anode (site where corrosion occurs and from which electrons flow) and a cathode (site to which electrons flow). In addition to the anode and cathode, for corrosion to proceed, two other basic elements are required: an electrolyte (a medium capable of conducting electric current by ionic current flow and characterised by a resistivity), and a metallic path (connection between the anode and cathode, which allows current return - as electrons e^- flow - and completes the circuit), see Figure 3.

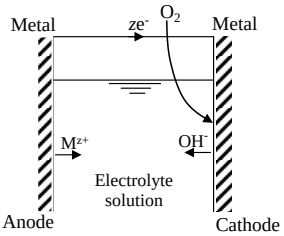

Figure 3: Basic corrosion process of a metal (Shreir *et al.*, 1994)

The equations governing the corrosion of a divalent metal, M (e.g. iron) in the presence of oxygen (O_2) can be simplified as follows:

$$\text{At the anode: } M \rightarrow M^{2+} + 2e^- \quad (1)$$

$$\text{At the cathode: } \tfrac{1}{2}O_2 + H_2O + 2e^- \rightarrow 2OH^- \quad (2)$$

During corrosion, chemical reactions in the cells cause a build-up of electrons at the anode, resulting in a potential difference between the anode and the cathode. If there is an electrical connection between the two, the electrons will flow towards the cathode where they are consumed in cathodic chemical reactions. The flow of electrons results in an electric current being generated.

c) Steel corrosion in concrete

Steel corrosion in concrete is a process in which iron is solubilised at the anode and oxygen is reduced at the cathode, with electrons flowing in the steel between anode and cathode. In reinforced concrete, the electrolyte is the alkaline pore solution while the steel bar serves as the metallic path between the anode and cathode. The anodes and cathodes are formed on the steel surface (Figure 4).

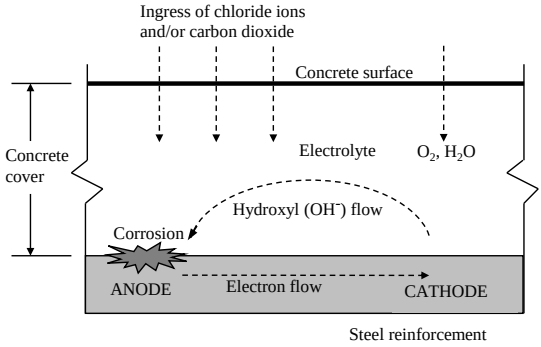

Corrosion reactions:

Anodic:

$$2Fe \rightarrow 2Fe^{2+} + 4e^- \quad (3)$$

Cathodic:

$$2H_2O + O_2 + 4e^- \rightarrow 4OH^- \quad (4)$$

Figure 4: A schematic illustration of the corrosion process in concrete

Steel passivation

Steel embedded in concrete is naturally protected against corrosion by the high alkalinity of the cement pore solution (pH > 12.5) and by the barrier effect of the concrete cover, which limits the oxygen and moisture required for active corrosion. The high pH suppresses steel corrosion by permitting the formation of a very thin (1-10 nm thick) passivating ferric oxide film (γ-Fe_2O_3) on the steel surface (Richardson, 2002). The passive layer on the steel can be disrupted or de-passivated by either a reduction in alkalinity (typically in carbonated concrete) or by chloride ingress (in marine concrete). De-passivation renders the steel thermodynamically

liable to corrode; whether it does so depends primarily on the availability of moisture and oxygen at the cathode.

Microcell and macrocell corrosion

Steel corrosion in concrete tends to be of two types: macrocell or microcell corrosion. Macrocell corrosion has a small anode and a large cathode which are clearly separated in different areas along the surface of the steel bar. This occurs frequently in chloride-induced corrosion in which concrete normally has a low resistivity (caused by the presence of chloride ions in the pore solution), and results in high localised corrosion (pitting corrosion) with large localised steel cross-section reduction.

In microcell corrosion, the anodic and cathodic sites are adjacent to each other, with multiple cells along the steel bar. This is more common in carbonation-induced corrosion in concrete, due to the normally higher resistivity of the carbonated concrete.

d) Assessment of reinforcement corrosion in concrete

This section briefly covers measurement parameters for corrosion. It is largely taken from Monograph 7 in this series (Mackechnie *et al.*, 2004). Specialised corrosion monitoring techniques are used to assess the probability of corrosion occurring, as well as the extent and severity of the problem. The more commonly used and accepted methods are briefly described below.

Half-cell potential measurements

This is an electrochemical method (also referred to as *open circuit* or *corrosion potential*) and is currently one of the most widely used methods for determining the probability of steel reinforcement corrosion in concrete. Corrosion of reinforcement is associated with anodic and cathodic areas along the reinforcement with consequent differences in electropotential of the steel. Rebar potentials are usually measured using a reference electrode connected to a handheld voltmeter, with an external attachment to the reinforcing steel (shown in Figure 5). This technique is better suited to chloride-induced corrosion than carbonation-induced corrosion where clearly defined anodic regions are not present.

The half-cell potential is a function of the extent to which steel is depassivated, and thus indicates the extent of carbonation or the presence of sufficient chlorides to break down the passive layer, as well as the pres-

ence of oxygen to sustain the passive layer. Half-cell potential measurements cannot evaluate the kinetics of the corrosion reaction and should only be used as an indication of the corrosion risk of the steel.

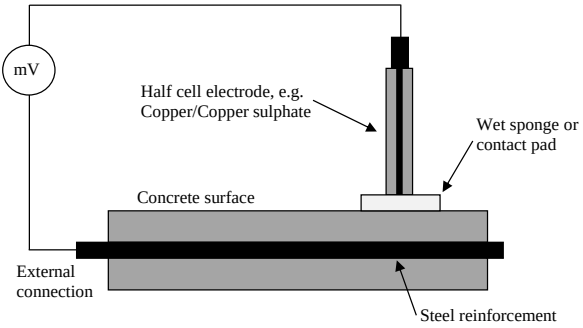

Figure 5: Schematic of half-cell electropotential measurement

Table 1 shows the ASTM guidelines for interpreting rebar potentials measured with either a copper/copper sulphate ($Cu/CuSO_4$) or silver/silver chloride (Ag/AgCl) half-cell (ASTM-C876-91, 1999).

Table 1: $Cu/CuSO_4$ and Ag/AgCl potentials and associated risk of corrosion (ASTM-C876-91, 1999)

Rebar potential (mV)		*Qualitative risk of corrosion*
$Cu/CuSO_4$ electrode	Ag/AgCl electrode	Likely corrosion condition
> – 200	> –106	Low (10% risk of corrosion)
– 200 to – 350	– 106 to – 256	Intermediate corrosion risk (uncertain)
< – 350	< – 256	High (> 90% risk of corrosion)
< – 500	< – 406	Severe corrosion

Resistivity measurements

Electrical resistivity is a measure of the ability of concrete to resist the passage of electrical current. Concrete resistivity therefore influences the corrosion rate of embedded steel once favourable conditions for corrosion exist.

The 4-point Wenner probe is commonly used to measure resistivity and consists of four equally spaced probes, which contact the concrete surface. This method, shown in Figure 6, uses a small alternating current that is passed between the two outermost probes, and the resulting poten-

tial difference between the inner two probes is measured to determine the resistivity of the concrete.

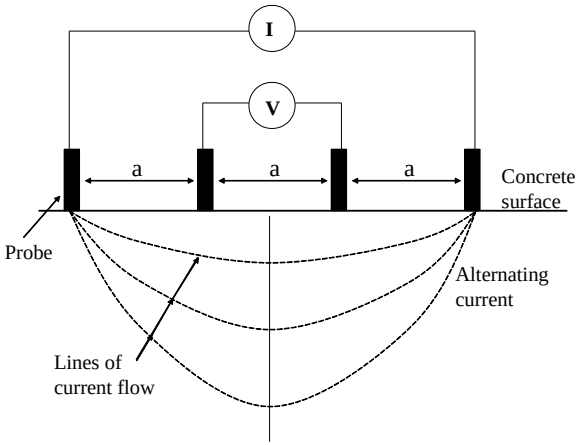

Figure 6: Principle of Wenner probe measurement of concrete resistivity

Table 2 provides an interpretation of resistivity measurements from the 4-point Wenner probe system, for de-passivated steel.

Table 2: Relationship between resistivity and corrosion risk (Andrade and Alonso, 1996)

Resistivity (kΩ-cm)	*Risk level*
> 100 – 200	Very low corrosion rate even if chloride contaminated
50 – 100	Low corrosion rate
10 – 50	Moderate to high corrosion rate
< 10	High corrosion rate; Resistivity is not the controlling parameter

Resistivity measurements should not be seen as definitive measures of corrosion activity but rather be used to complement other techniques.

Corrosion rate measurements

Corrosion rate, also known as corrosion current density, is a measure of the rate of electron transfer between the anode and cathode, and is designated i_{corr}. Corrosion rate measurements are the only reliable means of assessing corrosion activity in reinforced concrete. Corrosion rate (units of $\mu A/cm^2$) can be measured using a linear polarisation resistance (LPR) technique. This technique, also known as the polarisation resistance meth-

od, relies on the relationship between the half-cell potential of a piece of corroding steel and an external potential or current applied to it. Measurements are performed by applying a small potential (to perturb the reinforcing steel from its equilibrium potential) either as a constant pulse (potentiostatic), or a potential sweep (potentiodynamic), and measuring the current response. Alternatively, a current pulse (galvanostatic) or a current sweep (galvanodynamic) can be applied, and the potential response measured.

A further alternative is the coulostatic technique, whereby a small charge is applied to the steel surface and relaxation of potential is measured over a short period of time. Three electrodes are used: counter/auxiliary (e.g. stainless steel), working, and reference electrodes. The potential or current is applied to the embedded steel reinforcement (i.e. the working electrode) through the counter electrode while the reference electrode (e.g. Ag/AgCl) is used to measure the change in potential due to applied current or potential over a short period of time, typically one minute, to determine the polarization resistance R_P. The polarization resistance is then converted into a corrosion rate by means of the Stern-Geary relationship (see Equation 13 in the Appendix).

Corrosion rate measurements on field structures are most commonly done using galvanostatic LPR techniques with a guard-ring sensor to confine the area of steel under test. However, a coulostatic device was used for this work in the laboratory. Table 3 shows a qualitative guide for assessing corrosion rates of structures.

Table 3: Qualitative guide for the assessment of corrosion rates (RILEM TC 154-EMC, 2004)

Corrosion rate ($\mu A/cm^2$)	*Qualitative assessment of corrosion rate*
> 1.0	High
0.5 – 1.0	Moderate
0.1 – 0.5	Low
< 0.1	Passive (negligible)

e) Corrosion products

Iron (Fe) that has been converted to Fe^{2+} can then form corrosion products of hydroxides, oxides and oxide-hydroxides, depending on conditions of temperature, atmospheric pressure, potential and pH. These corrosion products occupy larger volumes than the original iron, as shown in Figure 7.

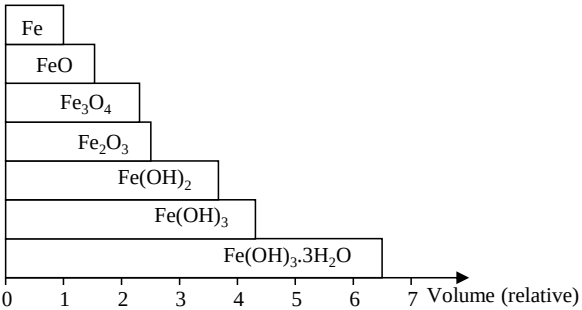

Figure 7: Relative volume of iron corrosion products (Liu, 1996)

It is this volume expansion that causes cracking and spalling in the concrete cover.

f) Corrosion of steel in cracked concrete

Reinforced concrete is frequently designed to act in a cracked state, and many RC structures exhibit load-induced and other forms of cracking from a relatively early age. In cracked concrete, corrosion typically starts either in the crack or in the area immediately adjacent to the crack.

Corrosion in cracked concrete tends to occur in two different ways: one where small anodic and cathodic sites are very close together in the zone of the crack (microcell corrosion) and the oxygen for the cathodic reaction is supplied through the crack; the other where the reinforcement in the crack acts as an anode and the passive steel surface between the cracks forms the cathode. In the latter case, oxygen penetrates through the uncracked concrete (macrocell corrosion), and since the cathodic steel surface is larger than in the first mechanism, higher corrosion currents occur (Schießl and Raupach, 1997).

The following sections deal with corrosion initiation and corrosion propagation and how these relate to service life of reinforced concrete structures.

CORROSION INITIATION

Carbonation of concrete or chlorides penetrating into concrete can both cause the steel (or part of it) to be de-passivated and start to corrode actively. This is called ‘corrosion initiation’. This monograph is concerned mainly with chloride-induced corrosion since it is invariably very perni-

cious and destructive to RC. However, carbonation-induced corrosion will also be covered briefly for completeness.

a) Initiation of carbonation-induced corrosion

Carbonation occurs in concrete when atmospheric carbon dioxide, CO_2, penetrates into the concrete by diffusion, and reacts mainly with the water and calcium hydroxide in the concrete to form calcium carbonate, $CaCO_3$. This results in the lowering of the pore solution pH from above 12 to between 8.5 and 9.0. The simplified carbonation reaction is as follows:

$$CO_2 + Ca(OH)_2 + H_2O \rightarrow CaCO_3 + 2H_2O \quad (5)$$

The reduced alkalinity leads to the de-passivation of steel in contact with the carbonated zones. The reaction front progresses in a step-wise fashion into the concrete. Once this carbonation front reaches the steel, the corrosion process begins, provided there is sufficient moisture and oxygen present. Carbonation usually induces a generalized (microcell) type of corrosion, where there are no distinct anodes or cathodes.

Carbonation is a diffusion process, generally modelled by the simplified expression:

$$x = k_{co_2}\sqrt{t} \quad (6)$$

where x = carbonation depth after time t

k_{co_2} = carbonation coefficient of the particular concrete

Carbonation progresses most rapidly in concrete with relative humidity values between about 40% and 70%. It does not occur if the concrete is water-saturated or in very dry conditions because, respectively, CO_2 is not readily soluble in water, and moisture is required in the reaction.

Increased carbonation rates also occur with increasing carbon dioxide concentration and at higher w/b ratios (i.e. w/b ratios at or above 0.6). Carbonation rate reduces by approximately 50% when the w/b ratio is reduced from 0.6 to 0.4 (Parrot, 1987). At equal w/b ratios, blended cement concretes (e.g. concretes incorporating fly ash or slag) have lower carbonation resistance owing to their lower $Ca(OH)_2$ content.

The most common method to measure carbonation depth is to spray a 1% phenolphthalein solution on to a freshly broken concrete surface.

Where the pH is greater than 9, the concrete turns purple with gradually lightening shades of pink for pH of 8-9. Colourless concrete represents the practical depth of carbonation where the pH is at or below approximately 8. Figure 8 shows a concrete specimen, in cut cross-section, with a carbonated top portion at the exposed surface of approximately one centimetre, the deeper portion being uncarbonated. (In colour, the top portion appears colourless while the bottom portion is coloured purple).

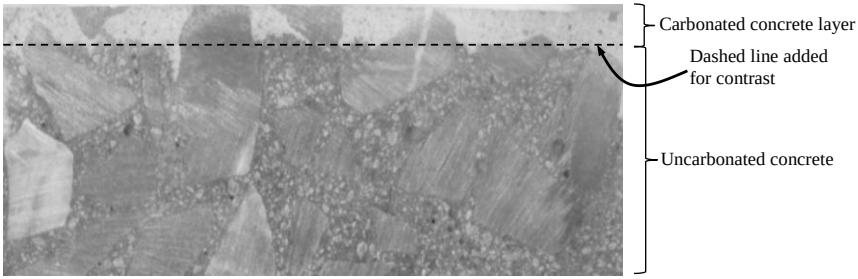

Figure 8: Cross-section of concrete showing the carbonated (outer) and uncarbonated (inner) zones

b) Initiation of chloride-induced corrosion

Chloride ions in sufficient concentration in concrete may de-passivate the steel locally by breaking down the protective layer of γ-Fe_2O_3. Chlorides (Cl^-) are not consumed in the corrosion process but they help to break down the passive layer and greatly accelerate corrosion. Chloride ions act as a catalyst for the oxidation of iron through the formation of the $FeCl_3^-$ complex which is unstable and can be drawn into solution where it reacts with the available hydroxyl ions to form $Fe(OH)_2$ (see Figure 9). This results in the release of Cl^- back into the solution and consumption of hydroxyl ions, as shown in the following equations:

$$2Fe + 6Cl^- \leftrightarrow 2FeCl_3^- + 4e^- \quad (7)$$

followed by:

$$2FeCl_3^- + 4OH^- \leftrightarrow 2Fe(OH)_2 + 6Cl^- \quad (8)$$

The resulting corrosion is usually of the macrocell type, causing intense localized pitting corrosion. The process is self-propagating, due to the

acidic conditions created and the recycling of chloride ions by hydrolysis of the chloride compounds. In addition, chlorides reduce the resistivity of the concrete, which results in higher corrosion rates.

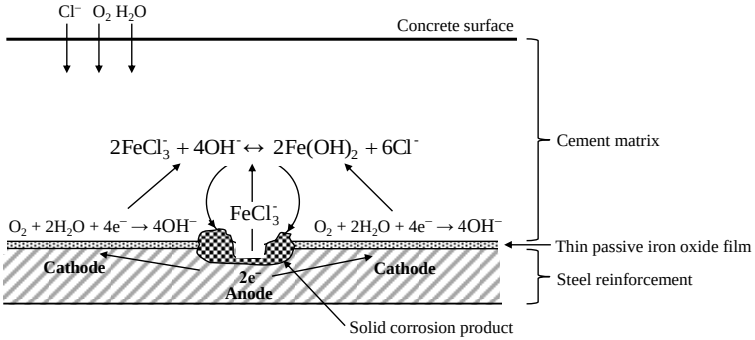

Figure 9: Corrosion of reinforcement in concrete exposed to chloride ions (Broomfield, 2007)

Passivity should not be viewed as a complete protection of the underlying metal but rather as a limiting value of corrosion. Indeed, some corrosion of the steel is required to form the passivating layer of oxide! Under normal conditions, the passive layer is in a continual state of breakdown and repair. Chloride ions contribute towards the breakdown of the passive layer while other anions such as OH^- are responsible for its stability and have inhibiting properties. There is a point therefore at which the concentration of aggressive ions overcomes the inhibiting ions and corrosion can initiate. This point is known as the chloride threshold level (see below), represented by the pitting potential, below which passivity is maintained (Bockris *et al.*, 1981).

Chloride threshold level

It was mentioned previously that 'sufficient' chlorides are needed at the steel surface to initiate corrosion. This chloride threshold level (or critical chloride concentration) is the concentration of chlorides necessary to break down the passive film on the steel surface and initiate corrosion. It is an important input parameter in service life prediction models.

The chloride threshold level is not a single value for all types of concretes, steels and environments, but is affected by factors such as cover thickness, temperature, relative humidity, electrical potential of the rein-

forcement, chemistry of the binder, proportion of total chlorides to free chlorides, and chloride to hydroxyl ion ratio. Since some of these factors change with time, the chloride threshold value may also change with time. All chlorides (both bound and free - see later) can potentially influence corrosion, and so it is usually the total chlorides in the concrete that are considered for the chloride threshold. Different approaches have been used to express the chloride threshold level. These include:

i) the proportion of free chlorides (an over-simplification)
ii) the ratio between free chloride and hydroxyl ion concentration, which expresses the ratio of aggressive to inhibitive ions influencing corrosion initiation. However, other factors such as the inhibitive effect of the cement matrix related to a denser hydration product layer on the steel surface are also important
iii) total chloride (acid soluble) content. This is the most widely used approach

Generally, a large scatter is found in the literature on the minimum total chloride content that is required at the steel to initiate corrosion. Values vary from 0.02 to 3.08% total chlorides by mass of binder. A conservative value of 0.4% total chlorides by mass of binder is given by most authors. The increased use of mineral extenders such as fly ash and slag also makes the prediction of the chloride threshold level in concrete difficult.

Effect of cement extenders on chloride threshold level

Cement extenders generally lower the chloride threshold level, attributed to the reduction in alkalinity and the presence of sulphides in any slag blended binders. In his doctoral research, Scott (2004) found varying chloride threshold values for concretes with different binders as shown in Table 4.

Table 4: Variation of chloride threshold level with binder type (Scott, 2004)

Binder Type	*Chloride threshold (% conc. by mass of binder)*
Plain Portland Cement (PC)	0.53
75/25 PC/GGBS	0.41
50/50 PC/GGBS	0.08
25/75 PC/GGBS	0.20
70/30 PC/Fly ash	0.36
50/43/7 PC/GGBS/silica fume	0.08

However, it must be stressed that different researchers have arrived at very different values for the chloride threshold level in concretes with different binders. For example, Thomas (1996) found that the threshold chloride value decreased with increasing substitution of PC by FA in reinforced concrete specimens after exposure to a marine environment for up to four years. Similarly, (Oh *et al.*, 2003) measured lower chloride threshold levels with increasing addition of FA. In comparison with PC, lower chloride threshold values have also been reported for silica fume (SF) - containing binders (Pettersson, 1995, Manera *et al.*, 2008). The partial replacement of PC with SF reduces the aluminate phases and thereby the ability of the cement to bind chlorides. However, since the addition of SF also leads to pore refinement, the effect of physical adsorption is more pronounced in SF-containing binders. Work by (Gouda and Halaka, 1970) gave lower chloride threshold values for specimens containing slag when compared to specimens containing PC. The use of GGBS increases the chloride binding capacity due to improved chemical and physical binding (Arya *et al.*, 1990, Dhir *et al.*, 1996, Luo *et al.*, 2003).

Lastly, low threshold values for the blended cements may also be attributed to the slow early hydration process leading to higher short-term concrete permeability. In the long term, the denser pore structure in these concretes tends to result in substantial decrease in corrosion rate or a stifling of the corrosion process.

Free and bound chlorides (chloride binding)

Not all of the chlorides in concrete are free or mobile and thus available for corrosion. Some are bound to the cement matrix. Free chlorides are those dissolved in the concrete pore solution, and their concentration reduces with time due to chloride binding. Binding is the removal of chloride ions from the pore solution through interaction with the cement matrix. Chlorides in concrete can be bound chemically through a reaction with the aluminate phases (C_3A and C_4AF) to form calcium chloroaluminates. They can also be physically bound to hydrate surfaces by adsorption (Boddy *et al.*, 1999). All cements bind chlorides to some degree and this strongly influences the rate at which chlorides penetrate into the concrete from an external source.

Bound chlorides exist in chemical equilibrium with the free chlorides, which means they can be released under certain conditions to become free chlorides again. Such a condition occurs when chloride contaminated con-

crete subsequently carbonates, which causes a release of the bound chlorides. Thus, bound chlorides also present a corrosion risk. While chloride binding retards chloride penetration, it also allows the build-up of higher chloride contents that can increase the corrosion risk in some situations. The nature of the cement chemistry is important in chloride binding. In exposure conditions where chlorides are a problem such as marine conditions, choice of binder type is critical.

Effect of chloride binding on corrosion initiation

The effect of chloride binding on corrosion initiation is twofold: (1) the rate of chloride transport in concrete is reduced by binding since the amount of mobile ions (free chlorides) is reduced and (2) the reduction of free chlorides results in lower amounts of chlorides accumulating at the reinforcing steel and therefore it takes longer to reach the chloride threshold level.

Cement extenders, which tend to bind chlorides more effectively, have a dramatic effect on time to corrosion initiation. For example, Tarek *et al*. (2002) examined concretes after 15 years of exposure in tidal zones. For a cover depth of 70 mm and a threshold value of 0.4% total chlorides by mass of cement, the time to corrosion initiation was found to be 22, 65 and 150 years for PC, FA (10-20%), and slag concretes (60-70%) respectively. Similar results were obtained by Mackechnie and Alexander (1996). However, the increased time to corrosion initiation cannot only be attributed to chloride binding effects, since other effects such as the denser pore structure in the blended cements may also contribute to the longer time to corrosion initiation.

Even after corrosion has started, the rate will continue to be affected by binding as there is a slower increase in chloride level which in turn limits the increase in corrosion rate.

Slag-blended concretes

Slag-blended concretes are particularly effective in reducing chloride-induced corrosion. Slags have higher aluminate contents than plain Portland cement, and this can enhance the chloride binding capacity, thereby decreasing the free chlorides and increasing the bound chloride content in concrete, which results in an extended corrosion initiation period. (The question of various sulphur species in slags is dealt with later).

c) Chloride ingress and time to initiation of chloride-induced corrosion

The corrosion initiation period (t_i) for chloride-induced corrosion is the time required for chlorides at the steel to reach the chloride threshold level and thereby trigger the corrosion process. Chloride ingress in concrete structures is influenced by the following aspects:

(i) The penetrability of the concrete, which is largely influenced by mix parameters (primarily w/b ratio and binder type), and construction procedures (e.g. compaction and curing)
(ii) The heterogeneous nature of concrete, such as the presence of cracks and interfacial transition zones (ITZ) between cement paste and aggregates
(iii) Surface chloride concentration that varies with time
(iv) Changing environmental conditions, such as temperature and humidity, which affect the rate of chloride ingress
(v) Hydration of cement paste, which continues after the structure is put in service and affects the rate of chloride ingress
(vi) Chloride binding, which occurs to varying degrees, depending on the binder type

The time to corrosion initiation depends on the chloride binding capacity of the binder, the chloride threshold value, thickness and condition of the concrete cover, and resistance of the cover zone to chloride ingress.

In relation to chloride-induced reinforcement corrosion, blended cement concretes have been found to clearly outperform concretes made with plain Portland cement. Figure 10 shows the results from the South African prediction model for chloride-induced reinforcement corrosion, for concretes made with 3 types of cementitious materials, cured for the first 3 days at 90% relative humidity, 60 mm cover depth and subjected to tidal zone conditions (Mackechnie, 1997). Although the assumed model input parameters may be somewhat subjective, the figure clearly shows the superior performance of blended cements in delaying the onset of rebar corrosion in concrete.

Equations for describing chloride ingress are normally based on diffusion theory. While this is not strictly correct, it serves as a useful starting point for prediction. Fick's second law of diffusion concerns the rate of change of concentration with respect to time (t) and spatial position (x) in a structure. For a semi-infinite homogeneous medium, the law may be stated as follows:

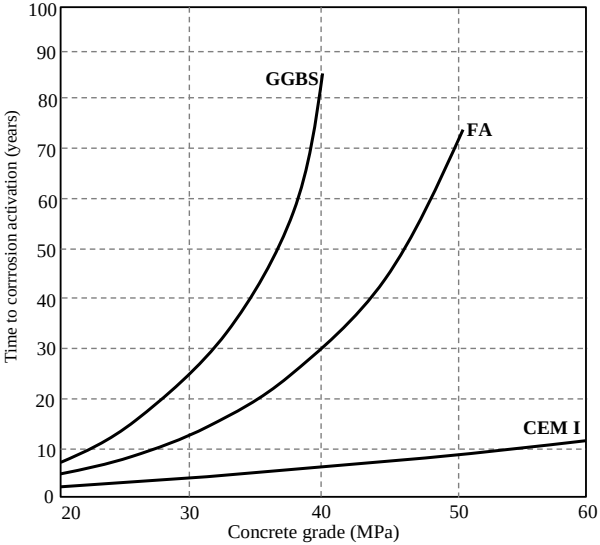

Figure 10: Model prediction results of the time to corrosion initiation for different concrete types (Mackechnie, 1997)

$$\frac{\partial C}{\partial t} = D\frac{\partial^2 C}{\partial x^2} \tag{9}$$

where D = diffusion coefficient
C = chloride concentration

The boundary conditions are given by:

C_x = 0 at $t = 0$ and $0 < x < \infty$
C_x = C_s at $x = 0$ and $0 < t < \infty$

where C_x = chloride concentration at depth x at time t
C_s = surface chloride concentration

Equation (9) is usually solved using Crank's error function:

$$C_{x,t} = C_s\left[1 - erf\left(\frac{x}{2\sqrt{Dt}}\right)\right] \tag{10}$$

where $C_{x,t}$ = chloride concentration at the depth x at a given time t
C_s = surface chloride concentration
D = chloride diffusion coefficient
t = time of exposure
erf = error-function

The above equations are 'ideal', i.e. they assume a time-invariable diffusion coefficient and surface chloride concentration, which is not the case in actual concrete structures. Nevertheless, for practical purposes, Fick's law can be used with reasonable accuracy. Reasons for the deviation from ideal conditions include intermittent contact of chlorides with concrete structures such as in the intertidal zone where the concrete is exposed to cycles of wetting and subsequent evaporation (drying). The other non-ideal condition is that the diffusion coefficient changes with time due to ongoing cement hydration and chloride binding. This means that an apparent diffusion coefficient D_a is usually used in the expressions. This time-dependent (or time-integrated) apparent diffusion coefficient is described by the relation:

$$D_a = D_o\left(\frac{t_o}{t}\right)^m \tag{11}$$

where D_o is the diffusion coefficient at some reference time t_o (e.g. 28 days)
m is the aging coefficient (reduction factor). The value of the aging factor depends mostly on the binder type.

Chloride profiles

Chlorides penetrate into concrete from the surface, their concentration increasing with time but reducing with depth. This variation with depth is called a chloride profile. It can be obtained experimentally and Fick's law essentially describes this profile. Figure 11 shows a typical experimental profile to which a line has been fitted based on Equation 10.

A feature of chloride profiles is often that near the surface, the profile does not follow the predicted shape because of surface wetting and drying cycles. The depth over which this occurs is termed the convection zone (Figure 12). Beyond the convection zone, diffusion is considered the deci-

sive transport mechanism. The data points in the convection zone are often neglected in profile curve fitting.

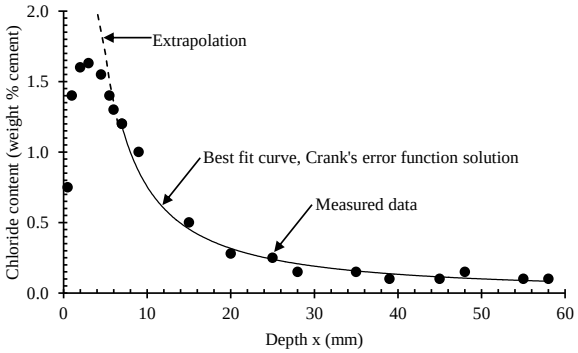

Figure 11: Typical chloride profile from splash zone (profile has been fitted to error function neglecting data points in the convection zone) (Hunkeler, 2005)

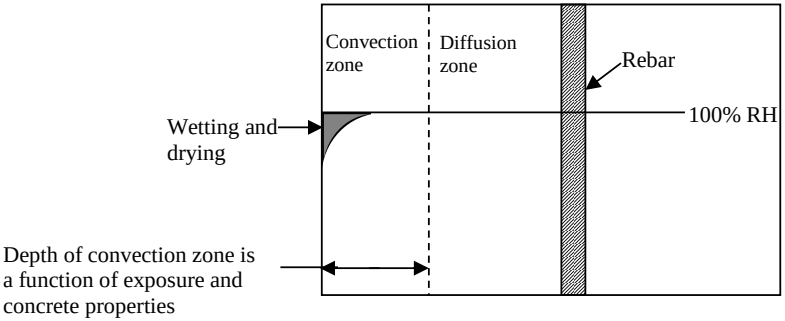

Figure 12: Convection zone in concrete (LIFE-365, 2005)

Chloride ingress prediction models

Some of the existing chloride ingress prediction models are briefly discussed here. As the name implies, they are used to predict the rate of chloride ingress into concrete and therefore serve as important aspects of service life models.

DuraCrete

DuraCrete (*Dura*bility design of con*Crete* structures (DuraCrete, 1998)) is a European design method that is explicitly based on performance, relia-

bility, and a design service life. It recognizes that the service life of structures is a stochastic quantity that can best be described in terms of probability. It follows the same principles of reliability and performance as structural design codes. In predicting the time to corrosion initiation or concentration of chlorides at a given time and depth in the cover, DuraCrete uses Crank's solution to Fick's second law but takes into account the variability of the input parameters i.e. diffusion coefficient, cover depth and chloride threshold level. It therefore requires realistic and accurate definitions of environmental actions, material parameters for concrete and reinforcement, mathematical models for degradation processes and mechanical behaviour, performance expressed as limit states, and reliability. Its main drawback is the need for large amounts of data to be able to quantify all the variables adequately for a specific environment.

ClinConc

ClinConc (*Ch*loride *in Conc*rete) is a Swedish performance-based numerical model (Tang, 1996) and is used mainly in the Scandinavian countries. It consists of two main procedures:

- Simulation of free chloride penetration through the concrete pore solution using a flux equation based on Fick's law and
- Calculation of the distribution of the total chloride content in concrete using mass balance combined with nonlinear chloride binding.

The model uses free chloride as the driving force and takes chloride binding into account, but needs numerical iterations for the binding effect, which limits its practical engineering applications. The model is also based on Crank's solution to Fick's second law of diffusion with the main input parameters being exposure conditions, cover depth and chloride diffusion coefficient obtained using the Rapid Chloride Migration test (Tang, 1996).

LIFE-365

LIFE-365 (2005) is a North American probabilistic computer-based simulation approach for service life prediction, and incorporates life-cycle cost functionality. It recognises that corrosion-induced damage can often be mitigated through many strategies including low concrete permeability, corrosion inhibiting admixtures, epoxy coated steel reinforcement, corrosion-resistant steel, application of waterproofing membranes or sealants, or combinations of these methods and materials. Each of these strategies

has technical merits and costs, and the challenge is to select the proper combination of protection methods, at an acceptable cost, to achieve the desired result. Many assumptions are made to simplify the model and hence the calculated service life and life-cycle cost obtained using this model should be considered in relative terms.

South African chloride ingress model

This is an empirical performance-based prediction model for RC in a marine environment developed by Mackechnie (1996). The model uses results of durability index tests (chloride conductivity) to characterise early age concrete properties and then relates these to the potential durability performance of the concrete exposed to a range of marine environments. The classification of the marine environments is based on EN 206-1 (2000), modified for South African conditions (Table 5) (Alexander and Beushausen, 2007). In short, the model is based on the relationship between early age properties, validated with long-term chloride ingress data from marine concrete structures.

Table 5: South African environmental exposure classes (after BS-EN-206-1, 2000) for chloride-induced corrosion

Exposure Class	*Description*
XS1	Exposed to airborne salt but not in direct contact with seawater
XS2a^{+}	Permanently submerged
XS2b^{+}	XS2a + exposed to abrasion
XS3a^{+}	Tidal, splash and spray zones
XS3b^{+}	XS3a + exposed to abrasion

$^{+}$ These sub-clauses have been added for South African coastal conditions

CORROSION PROPAGATION

The monograph deals with the experimental work on corrosion propagation in cracked concrete later in Part II; this section gives a brief overview of the basics of corrosion propagation.

Figure 2 defines the propagation phase as the period following corrosion initiation, when damage begins to occur in the structure. Considerable chloride ingress has already occurred and the structure must now be managed for the consequences of damage. Corrosion propagation is characterised by active corrosion and usually leads to cracking, delamination, and spalling of concrete cover due to expansive corrosion products. Nev-

ertheless, with suitable repair and maintenance strategies, the propagation phase can be extended to give useful structural performance.

It is important to distinguish between the *thermodynamic* and the *kinetic* aspects of corrosion. Once corrosion initiates due to favourable thermodynamic conditions (i.e. the chloride threshold level is exceeded), the kinetics or the rate of corrosion is subsequently governed more by the availability of oxygen and the electrical resistivity of the system. Oxygen and moisture are the 'fuel' for the corrosion process. Conventionally, corrosion rates below 0.1 $\mu A/cm^2$ are taken as representing a passive corrosion state, whereas higher rates characterise active corrosion. Therefore, a corrosion rate of 0.1 $\mu A/cm^2$ is taken as the transition point from passive to active corrosion and as the start of the propagation phase (see Table 3).

a) Factors affecting corrosion propagation due to chloride-induced corrosion

Cement extenders

Apart from having an influence on corrosion initiation, cement extenders such as slag, fly ash and silica fume also have a profound effect on the rate at which corrosion progresses (Mangat *et al.*, 1994, Mackechnie and Alexander, 1996). This is largely due to the higher resistivity that extenders impart to concrete (see later). Part II of this monograph will give further information on this aspect in relation to local research.

Moisture content and relative humidity

Moisture content in concrete is an important factor for both corrosion initiation and propagation. For corrosion initiation, it influences the ingress of oxygen; further, chlorides can only diffuse through moist or saturated concrete. In the propagation phase the corrosion rate is slow in dry or fully saturated concretes; intermediate moisture contents allow the concrete to act as an electrolyte while also permitting the ingress of oxygen needed for the corrosion process.

Active corrosion can therefore not occur if the concrete is too dry such that the pore solution does not serve as an electrolyte, or too wet (saturated) to allow ingress of oxygen. Corrosion activity is most vigorous at relative humidity (RH) values above about 80% (Richardson, 2002). Concerning the rate of ingress of oxygen to the cathodic areas, this depends on its diffusion coefficient, the depth of the steel, and the condition of the cover concrete. The diffusion coefficient is affected by the w/b ratio and the

moisture content or relative humidity of the concrete. The oxygen diffusion coefficients for two w/c ratios of cement paste at various RH are shown in Figure 13.

Temperature

Steel corrosion rate in concrete is increased by high temperature and high humidity. Generally, corrosion rate increases up to a temperature of about 40°C followed by an inhibiting effect above this temperature, caused by the decreasing oxygen solubility in the pore solution at higher temperatures, and by the concrete progressively drying out if moisture is not readily available (Zivica, 2003).

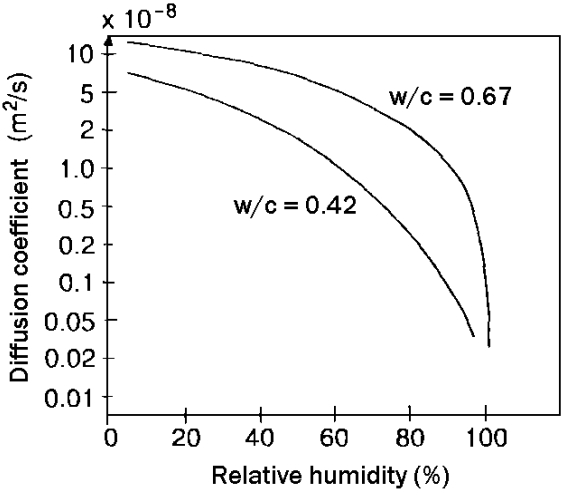

Figure 13: Influence of w/c ratio and RH on the oxygen diffusion coefficient (Bentur *et al.*, 1997)

Water/binder ratio and binder content

For concrete in a moist environment, the cathodic reaction depends on the availability of oxygen at the cathode, and the corrosion rate may therefore be limited by the cathodic reaction. With a decrease in w/b ratio, oxygen ingress decreases due to lower concrete permeability, thus suppressing the cathodic reaction. Also, the concrete resistivity increases with a decrease in the w/b ratio. Corrosion rate may also be controlled by the alkalinity, which is higher in concrete that has a lower w/b ratio.

Corrosion rates for 12 mm deformed steel in concrete prisms (100 x 100 x 370 mm) exposed to 1200 wetting and drying cycles in a sea-water spray chamber after 14 days air-curing, with a cover of 10 mm and three different w/b ratios and cement contents, were examined by Mangat *et al*. (1994). The results are given in Table 6.

Clearly w/b ratio had a more significant impact on the corrosion rate than cement content. The highest corrosion rate was observed in the 0.76 w/b ratio with the accompanying highest chloride concentration, while the lowest corrosion rate was found in the 0.45 w/b specimen despite having higher chloride content than the 0.58 w/b with 530 kg/m^3 cement. The effects of the material are thus significant beyond simply limiting the chloride ingress.

Table 6: Influence of w/b and cement content on corrosion rates (Mangat *et al.*, 1994)

w/b	*Cement* (kg/m^3)	i_{corr} ($\mu A/cm^2$)	*Acid soluble* Cl^- *at steel level (10 mm) (% by mass of cement)*
0.45	430	0.13	1.4
0.58	430	0.65	2.0
0.58	330	0.62	1.7
0.58	530	0.52	1.2
0.76	430	2.16	2.3

Concrete resistivity

Concrete electrical resistivity is a measure of the ability of concrete to resist the passage of electrical current. Corrosion of steel in concrete, being an electrochemical process, can be electrolytically stifled by a dry or impermeable material. Concrete resistivity therefore influences the corrosion rate of embedded steel once favourable conditions for corrosion exist. High resistivity will reduce corrosion currents and slow the rate of corrosion. Thus, the corrosion current density (or corrosion rate) is inversely proportional to the resistivity of concrete (or directly proportional to its conductivity) (Hunkeler, 2005):

$$i_{corr} \approx \frac{1}{R_c} = \sigma_c \qquad (12)$$

where: i_{corr} = corrosion current density ($\mu A/cm^2$)

R_c = concrete resistivity

σ_c = concrete conductivity

Resistivity depends on the moisture condition of the concrete, permeability and diffusivity of the microstructure, and on the concentration of ionic species in the pore solution. It is thus influenced by many factors including binder type and content, w/b ratio, degree of pore saturation, type of aggregate, presence of salts such as chlorides, temperature and age of the concrete and physical pore structure.

The electrical resistivity of concrete may vary over a wide range, from 1 kΩ-cm to 10^4 kΩ-cm. A resistivity of less than 5 kΩ-cm can support very rapid corrosion of steel, but if the electrolyte has high resistance to the passage of current, or if the concrete is dry and unable to support ionic flow, then corrosion will occur only at a very slow rate. Therefore corrosion can be limited by increasing concrete resistivity. Table 2, given earlier, indicates that resistivity can be used as an indirect measure of the probability of corrosion propagation.

Concrete cover thickness

The thickness and quality of the concrete cover influence the ingress of chlorides and oxygen into the concrete. The effect of cover on the diffusi-

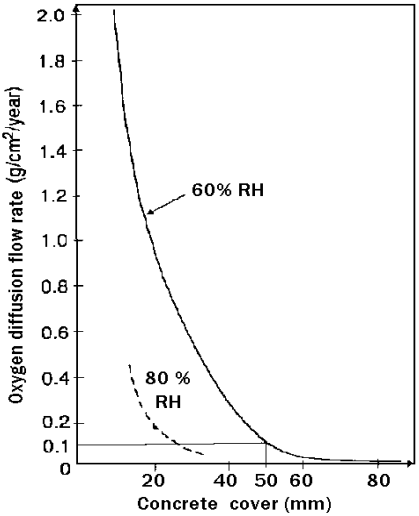

Figure 14: Effect of concrete cover on the diffusion of oxygen (Bentur *et al.*, 1997)

on of O_2 is shown in Figure 14, indicating how even a small increase in cover can have a large influence on oxygen ingress. A shift in relative humidity from 60 to 80% also results in a substantial decrease in the availability of O_2. On the other hand, increased cover depth is also likely to minimize the influence of any external drying at the level of the steel thus sustaining a high relative humidity.

Concrete cover therefore affects the corrosion rate mainly by governing the travel path of the corrosion agents (oxygen, moisture, chlorides). Corrosion may be significantly inhibited during the service life of a RC structure if w/b ratio, cover, binder type and binder content are carefully chosen (and implemented). In practice, the predominant reason for premature reinforcement corrosion is often a lack of sufficient concrete cover, either due to design inadequacies or poor construction.

b) Influence of cracking on corrosion

Cracks in RC structures are inevitable and arise in all stages of their lives. The effects may range from trivial to catastrophic. Cracks may appear at the surface but may not penetrate the depth of a member. Some cracks may not be visible to the naked eye but nevertheless influence properties such as permeability. A further factor is autogenous healing where, in the presence of moisture and provided cracks are small and non-active, they may seal with time.

Structural design codes specify allowable crack widths, normally to protect against corrosion. They also give formulae for calculating crack widths, but it is known that these formulae may not be very accurate. Thus, the question of permissible crack widths is a difficult one due to the complex interrelations between concrete cover, exposure conditions, type of binder, etc. Maximum permissible crack widths are usually stated in codes and specifications for the design of reinforced concrete structures exposed to aggressive chloride environments. Some of these include ACI Committee 224 (2001): 0.15 mm, JSCE (1986): 0.15 mm, and EN 1992-1-1 (2004): 0.3 mm. However, conventionally, 0.4 mm is generally taken as the limiting crack width, below which corrosion may proceed similar to uncracked concrete (fib Model Code, 2010). Two types of cracks are of interest in respect of their link with corrosion: those present before the onset of corrosion which might enhance the corrosion processes, and those produced as a direct consequence of corrosion. We are concerned here with the former.

Cracks generally do not affect the load-carrying capacity of the concrete structure but adversely affect its durability by providing easy access for aggressive agents, especially chlorides in marine environments. Cracks in concrete cause localised chloride ingress and hence localised steel corrosion. The effects of cracks vary not only with their depth, but also with their width, frequency, orientation (relative to the steel reinforcement), and whether the cracks are active or dormant. These factors will be briefly covered in the following sections.

Crack width

There is conflicting evidence in the literature on the relationship between crack width and corrosion. Researchers such as Beeby (1983), Arya and Wood (1995) and Bentur *et al*. (1997) indicate that for reinforced concrete specimens that differed only in crack width, the time required to initiate corrosion was shorter for those with wider cracks, but the corrosion rates were not significantly influenced by crack width. In this school of thought, factors such as whether cracks are active or dormant, concrete properties (e.g. permeability), and environment are more important than crack width. Others contest this by indicating that cracks accelerate both corrosion initiation and propagation, but this is dependent on the concrete quality (w/b ratio and binder type) and cover depth (Suzuki *et al.*, 1990, Pettersson and Jorgensen, 1996, Scott and Alexander, 2007). What is clear is that pre-existing cracks result in much faster chloride ingress to the steel, such that the corrosion initiation phase may be effectively eliminated.

Notwithstanding these arguments, the concept of a critical crack width threshold exists, whereby it is assumed that, below this threshold width (typically taken as 0.4 mm), corrosion is limited or negligible. This aspect will be examined in more detail with reference to local research later in Part II.

Crack frequency

Crack frequency (or crack density) refers to the number of transverse (with respect to the orientation of the rebars) surface cracks per unit length. Where many surface cracks exist, crack frequency may be more important than crack width. This is seen in Figure 15 which shows a plot of the cumulative mass loss of steel vs. time for different crack frequencies. Clearly, corrosion rate increases with an increase in crack frequency.

This can be attributed to the increase in the permeability of the concrete, and hence ease of chloride ion ingress and oxygen into the concrete. (The specimens with the highest crack frequency of 20 did not correspond to the highest corrosion rate, which seems strange).

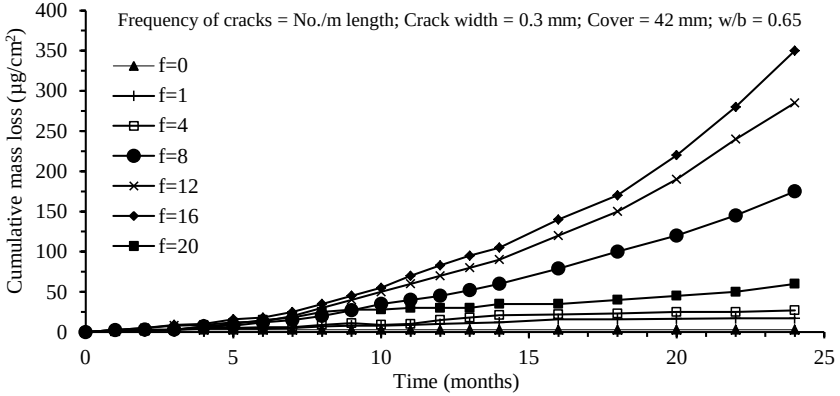

Figure 15: Effect of crack frequency on cumulative mass loss due to corrosion (Arya and Ofori-Darko, 1996)

Crack orientation

Orientation of cracks with respect to reinforcement is a very important factor influencing crack-induced corrosion. Cracks can be either longitudinal (coincident) or transverse (intersecting). Longitudinal cracking is extremely detrimental, since chlorides, moisture, and oxygen can easily penetrate to the embedded steel and attack large areas of steel in the corrosion process. For transverse cracks, the cathodic areas mostly occur in the uncracked regions. Therefore, moisture and oxygen that enter through the cracks may be expected not to greatly affect the rate of corrosion.

However, results of an experimental study by Otieno *et al*. (2010a) show that this is dependent on concrete quality (binder type and w/b ratio), as discussed in Part II of this monograph.

For concrete in service, transverse cracks are more likely in tensile-stressed areas of a RC structure. Longitudinal cracks are more associated with corrosion cracking along the longitudinal reinforcement due to the expansive nature of corrosion products. Restrained deformations in concrete such as thermal deformations and shrinkage may result in both

transverse and longitudinally cracked sections, however often with relatively low crack widths.

Crack dormancy or activity

Cracks in reinforced concrete structures can be either active or dormant depending on whether they frequently open and close (i.e. active) or not (i.e. dormant). The opening and closing of cracks can be due to application and removal of loads, for example in roads and bridges. It is very important to consider these phenomena because they can determine whether a crack can undergo self-healing (also called autogenous healing), a process which decreases the severity of cracks by decreasing concrete penetrability and hence improving the protection of the embedded steel from corrosion (Neville, 2002, Li and Li, 2011). The most significant factor which influences self-healing is the precipitation of calcium carbonate crystals in the cracks, as a result of $Ca(OH)_2$ leaching (Schießl and Edvardsen, 1993). Other causes of crack self-healing include swelling and hydration of cement paste, ettringite formation, and blocking of the crack by impurities in water and concrete particles (debris) broken from the crack surface (Edvardsen, 1999).

Other factors

Other factors that influence corrosion rates in cracked RC structures include cyclic wetting and drying which can accelerate corrosion rates by concentrating chloride ions in the surface zone, and sustained loading and loading history where it has been shown that steel under tensile stress corrodes faster than when unstressed. However, these are outside the scope of this monograph.

c) Prediction of the corrosion propagation period

The corrosion propagation period can be thought of as the time necessary for sufficient corrosion to occur to cause unacceptable damage to the RC structure, e.g. cover cracking. The length of this period depends on the definition of *unacceptable damage* or an *acceptable limit state*. This level of damage will vary depending on the requirements of the owner and the nature or use of the structure. For example, ACI committee 365 (2005) defines the propagation period as the *time to first repair*.

Assuming a certain damage limit state, the propagation period depends principally on the corrosion rate. The limit state may be described in terms

of parameters such as loss of steel cross sectional area, time to cracking, and loss of steel/concrete bond (Andrade and Alonso, 1996). Regarding loss of steel cross-sectional area, Andrade and Alonso (1996) suggest a value of between 5% and 25% to define the end of service life. Corrosion rate and loss of cross section are related through Faraday's Law.

Concerning time to corrosion-induced cracking, this cracking tends to run longitudinally with the steel and allows for a significant acceleration of the corrosion rate as the steel is more directly exposed to the atmosphere. Thus the onset of corrosion-induced cracking may also provide a reasonable, though conservative, estimate to the end of a structure's life and can be used to estimate the propagation period (Liu and Weyers, 1998). Several models have been developed to predict the time to cracking, relying on, for example, critical volume of corrosion products to induce cracking, and mean corrosion current. Further details may be obtained from the literature (Andrade *et al.*, 1993, Molina *et al.*, 1993, Alonso *et al.*, 1998, El Maaddawy and Soudki, 2007).

PART II: EXPERIMENTAL STUDIES ON CORROSION IN CRACKED AND UNCRACKED REINFORCED CONCRETE IN CHLORIDE ENVIRONMENTS

Part II of the monograph covers experimental results of Scott and Otieno, who studied corrosion initiation and propagation in RC members subjected to chloride exposure. It commences with a short section on simulated pore solution studies of steel corrosion, to highlight the important chemical factors particularly with regard to slag cements. Information is then given on corrosion rates in cracked and uncracked concretes based on experimental work, covering the influence of crack width and the important role of binder type in cement blends. Finally, the findings are generalised so as to give engineers a better understanding of how to deal with these problems in design and practice. Table 7 gives a summary of notations used to denote concrete mixes used by Scott and Otieno in their experimental studies. These are frequently referred to in this part of the monograph.

Table 7: Concrete mix notations

Notation	*Meaning*
PC–40	Concrete made with 100% plain Portland Cement (PC, CEM I 42.5N) at a w/b ratio of 0.4
PC–55	Concrete made with 100% PC at a w/b ratio of 0.55
PC–58	Concrete made with 100% PC at a w/b ratio of 0.58
SL_C–40	Concrete made with 50/50 PC/Corex slag blend at a w/b ratio of 0.4
SL_C–55	Concrete made with 50/50 PC/Corex slag blend at a w/b ratio of 0.55
SL_B–58	Concrete made with 50/50 PC/Ground granulated blast furnace slag (GGBS) blend at a w/b ratio of 0.58
FA–58	Concrete made with 70/30 PC/Fly ash (FA) blend at a w/b ratio of 0.58
SF–58	Concrete made with 93/7 PC/Silica fume (SF) blend at a w/b ratio of 0.58
TR–58	Concrete made with 50/43/7 PC/GGBS/SF blend at a w/b ratio of 0.58

PC (Portland cement) refers to CEM I 42.5N.

A summary of the concrete mix proportions can be found in the Appendix (Tables 13, 14).

A. SIMULATED PORE SOLUTION STUDIES OF STEEL CORROSION

INTRODUCTION

In simulated concrete pore solution studies, the ionic concentrations of the various species in pore solutions are determined, such as hydroxide (OH^-), chloride (Cl^-) and the various cations (mainly Ca^{2+}, Na^+, K^+). These species are important for their fundamental influences on steel corrosion in concrete and for the long-term performance of concrete. Concrete can be thought of as an electrolyte with embedded steel in which corrosion cells may be set up under certain conditions. Thus, the ionic composition of the electrolyte, i.e. the pore solution, is important in respect of steel corrosion.

Much can be learnt about basic mechanisms of corrosion from studying corrosion of steel in simulated pore solutions. One insight is that it is often the competition between different ionic species that influences corrosion and corrosion rates. For example, there is competition between hydroxide and chloride ions for reaction sites on the steel surface. At a certain critical concentration of chlorides - the so-called chloride threshold - corrosion initiates because at this critical chloride level, the passivating effect of hydroxide ions is broken down by the chlorides competing for reaction sites.

The inclusion of cement extenders in concrete results in a progressive reduction of hydroxide ion concentration with increasing replacement levels. Figure 16 shows that beyond about 28 days of hydration, hydroxyl ion concentration in the pore solutions is in the order from highest to lowest of PC–58 > SL_B–58 > FA–58 > TR–58 ≈ SF–58. On this basis, plain Portland cement concrete should provide the best protection against corrosion in view of its high hydroxyl ion concentration which, as indicated previously, helps to establish and maintain the passive layer on the steel. However, much depends on whether one is dealing with carbonation-induced corrosion or chloride-induced corrosion. For the latter, other factors such as resistivity and w/b ratio are far more influential than OH^- concentration *per se*, as will be seen later. In fact, it is essential to also study corrosion in the 'real' material concrete, since other physical and physico-chemical factors often override the effects of pore solution chemistry.

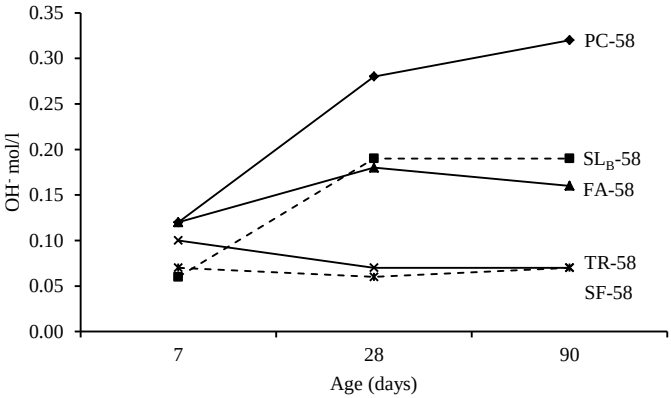

Figure 16: Influence of cement extenders on hydroxyl ion concentration (Scott, 2004)

a) Slag cements

Slag cements are important in modern binder technology, and generally help to improve concrete properties, particularly durability. One feature of slag cements is the oxygen reducing nature of their composition, associated with the presence of soluble sulphides such as S^{2-}, HS^{-}, and S_n^{2-}, even though total sulphide content of the slag may typically be less than 1% by mass (Pal *et al.*, 2002). The reducing character of slags can influence the electrochemical potential of slag-PC paste pore solutions.

Sulphides affect the steel in two ways:

(i) The sulphides are oxidized to sulphate SO_4^{2-}, and thiosulphate ($S_2O_3^{2-}$) by the available oxygen, thus depleting the oxygen concentration at the steel and creating a potentially reducing environment. The tendency is for sulphide species to predominate at early ages, and then to oxidise to sulphate and thiosulphate (ultimately all to sulphate), assuming there is sufficient dissolved oxygen.

(ii) The sulphides form a precipitate of FeS on the steel surface thus negatively affecting the formation of the passive oxide layer.

The depletion of oxygen in the presence of sulphides limits the formation of the passive layer on the steel surface, because the development of this layer depends on the availability of oxygen to sustain the cathodic reaction. The embedded steel may therefore be more susceptible to corrosion and, with the availability of corrosive agents such as chlorides, time to corrosion initiation may be decreased.

Thus, at early ages in slag systems, there is a competition between species regarding the formation of the passivating layer on the steel. Normally the dissolved oxygen helps form the passivating ferric oxide layer on the steel, but it is often used up preferentially to oxidise the sulphides. This results in rapid lowering of the dissolved oxygen, which compromises the early formation of the passivating layer. Subsequently however, provided oxygen can diffuse to the steel from the surface, the passivating layer is formed. The competition between dissolved oxygen (DO) and TRS (where TRS is the Total Reduced Sulphur, a combined measure of the various sulphur species) is shown in Figure 17.

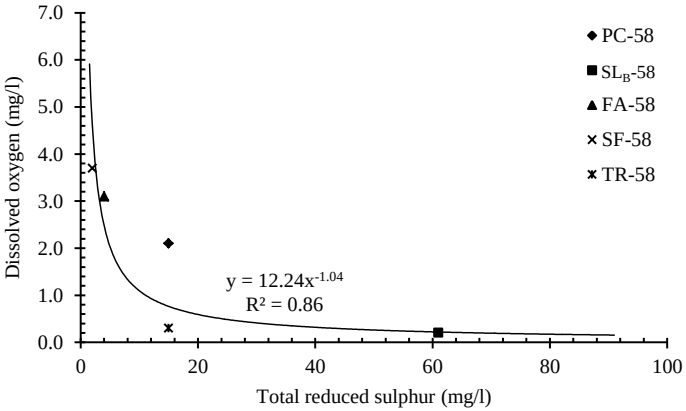

Figure 17: Relationship between DO and total reduced sulphur for 90 day results (Scott, 2004)

Table 8 shows measured TRS and DO. Clearly, PC–58 and FA–58 have low TRS levels, SF–58 virtually zero sulphides, while slag blended cements (SL_B–58 and TR–58) give high TRS values but correspondingly low dissolved oxygen. In ternary blended cements such as slag and silica fume blends with Portland cement, the two blending components may have different effects depending on the blending ratios. In general silica fume will depress the hydroxide ion concentration while the slag will have high TRS values, both of which might be expected to result in higher corrosion rates of embedded steel. However, as seen later, this is not necessarily the case from studies on actual concretes. Nevertheless, reduced hydroxyl ion concentrations and limited dissolved oxygen coupled with high levels of sulphur species in slag concretes may certainly result in lower chloride threshold levels as will be seen later.

Table 8: Concentrations of reducing sulphur species TRS and dissolved oxygen DO (mg/l) (Scott, 2004)

	7 day		*28 day*		*90 day*	
Mix	*TRS*	*DO*	*TRS*	*DO*	*TRS*	*DO*
PC–58	11	2.20	16	0.14	15	2.10
SL_B–58	50	0.06	106	0.10	61	0.10
FA–58	2	2.24	14	1.40	6	3.17
SF–58	0	2.75	3	3.40	2	3.70
TR–58	24	0.09	14	0.10	13	0.40

b) Steel corrosion in simulated pore solutions

Scott investigated steel corrosion in simulated pore solutions based on the various cement blends. He divided these into sulphide-free pore solutions (PC–58, FA–58 & SF–58) and sulphide-bearing solutions (i.e. slags). He allowed the passive layer to initially form on the steel by oxygenation prior to introducing corrosion-inducing chlorides.

In confirmation of the aqueous phase pore solution work, the sulphides were rapidly oxidised after the introduction of oxygen, with a corresponding increase in concentration of thiosulphate. Nevertheless, in sulphide-bearing solutions, it was clear that the development of the passive layer was retarded in comparison with sulphide-free specimens, shown by elevated initial corrosion rates and lower corrosion potentials prior to the introduction of chlorides.

Chloride threshold values in terms of Cl^-/OH^- ratios were studied on concrete specimens with w/b of 0.58. These varied as follows: sulphide-free: PC–58 = 1.21; FA–58 = 0.60; SF–58 = 1.39; sulphide-bearing: SL_B–58 = 0.51; TR–58 = 1.11. The presence of sulphides lowers the chloride threshold level (although FA also had a relatively low value).

Thus, the inclusion of sulphur species as in slag cements reduces the effectiveness of the passive layer in resisting the onset of active corrosion due to chlorides, according to this type of study. It was also clear that corrosion initiation is not simply a function of Cl^-/OH^- ratio, but also of the total hydroxide and chloride concentration. For example, a 4.8 times decrease in hydroxyl concentration resulted in a 15.5 times increase in corrosion rate at a chloride concentration of 0.2 M. The relative performance in terms of corrosion rates in the pore solution studies was, from highest corrosion rate to lowest: TR–58 > SF–58 > SL_B–58 > FA–58 > PC–58.

Importantly, the picture that emerges above was found to be in contrast to the situation of steel corrosion in actual concrete, due to physical effects such as relative humidity, porosity, and resistivity to name a few. *This is crucial since studies based solely on aqueous phase corrosion are sometimes used to justify concrete design rules.* The following sections of the monograph will show the effects in actual concrete in order to convey a fuller picture of the phenomena.

B. CORROSION RATE STUDIES IN CRACKED AND UNCRACKED CONCRETE

INTRODUCTION

This section summarises work done on corrosion in cracked and uncracked reinforced concrete beams by Scott (Scott, 2004) and Otieno (Otieno, 2008). Scott's work investigated both plain and blended cement concretes with cover to steel as a variable, while Otieno was more concerned with characterising the influence of a range of crack widths in plain and slag blended concretes. Their work is complementary. Brief details of the experiments and a summary of the main findings are presented first. Then, some of the detailed findings are presented to highlight the important influences. Finally, the results are generalised in order to draw insights for design and practice.

The work reported below should be viewed in the light of the fundamentals of steel corrosion that were presented in Part I of this monograph, as well as the pore solution studies presented in A. of Part II.

SUMMARY OF EXPERIMENTAL WORK AND MAIN FINDINGS

This section provides a summary of the experimental work done by Scott and Otieno relating to chloride-induced corrosion in cracked and uncracked concrete. More details on the experimental arrangements are provided in the Appendix.

Scott (2004) studied different binder types (PC, GGBS, fly ash, and silica fume) in small concrete beams (375 x 120 x 120 mm) with surface crack widths of 0.2 mm and 0.7 mm. Cracks were produced by bending of the specimens and allowing slipping of the embedded plain round rebars. A 5% NaCl solution was used to accelerate corrosion on the cracked face, while the w/b ratio was kept constant at 0.58. Two different concrete co-

vers (20 mm and 40 mm) were used. The main conclusions from the study were:

- Binder type, crack width and cover thickness all affect the corrosion rate of steel
- PC concrete had significantly higher corrosion rates compared to concrete made with cement extenders
- The concrete specimens containing 50% slag showed the best performance, i.e. the lowest corrosion rates
- Generally, the corrosion rate increased as the cover thickness decreased - see Table 9.

Table 9: Influence of crack width and cover on corrosion rate (Scott and Alexander, 2007)

Binder type	*Corrosion rate ($\mu A/cm^2$)*			
	0.2 mm crack width		*0.7 mm crack width*	
	20 mm cover	*40 mm cover*	*20 mm cover*	*40 mm cover*
PC–58	2.65	1.20	3.23	1.48
SL_B–58	0.39	0.35	0.51	0.53
FA–58	0.64	0.39	0.71	0.50
SF–58	0.67	0.59	1.12	1.03
TR–58	-	0.28	-	0.42

- For PC concrete, at constant crack widths of 0.2 mm or 0.7 mm, a decrease in concrete cover resulted in a significantly higher increase in corrosion rate compared to concrete made with blended cements. The effect of concrete cover depth on corrosion rate of PC concretes is therefore profound, other factors being constant
- For a constant concrete cover, increasing the surface crack width for a given concrete cover resulted in higher corrosion rates. This is expected because, at a constant cover, increasing the surface crack width results in a greater steel surface being exposed, assuming the crack is wedge-shaped.

The important overall conclusion from Scott's work is that corrosion rates in plain Portland concretes are much more sensitive to cover depth than in blended cement concretes.

Otieno (2008) studied concretes using two w/b ratios (0.40 and 0.55), two binder types (PC and 50/50 PC/Corex slag) and a constant cover of

40 mm. Crack widths were varied from 0 (uncracked) to 0.7 mm, including an 'incipient' crack, i.e. a crack just induced in the beam before unloading. The crack widths were maintained using a loading rig (see Appendix). Two crack reloading (re-opening) actions were also carried out, discussed in the next section. The main conclusion from Otieno's work was that the corrosion rate increased with increasing crack width, with even incipient cracks having a marked influence, the effect being more pronounced in plain concretes. Results are summarised in Figure 18.

Other conclusions from Otieno's work were:

- The presence of a crack increases corrosion rate by increasing concrete penetrability. The wider the crack, the higher the corrosion rate. However, the effect of cracks on corrosion rate is modified by concrete quality.
- Corex slag concretes (where corrosion rate tends to be governed by the high concrete resistivity) are less sensitive to the effects of cracking compared to PC concretes (with low concrete resistivity).
- Corex slag concretes are considerably less sensitive to changes in w/b ratio compared to PC concretes.

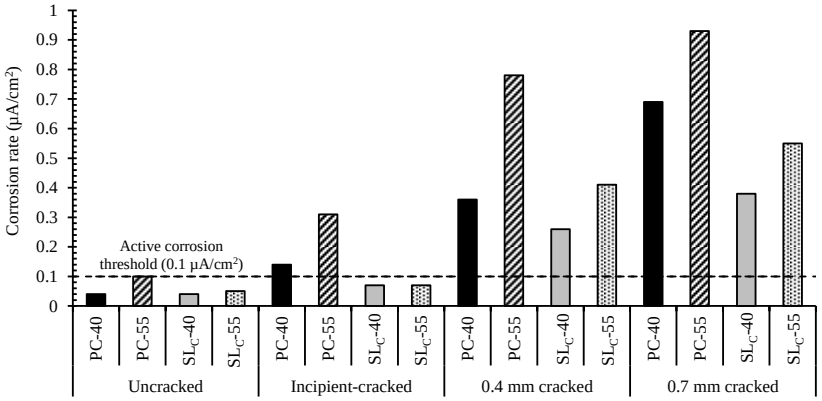

Figure 18: Mean corrosion rates for different binders, w/b ratios and crack widths (Otieno, 2008); Incipient crack - a crack just induced by 3-point loading of beam specimens and thereafter unloading. Constant cover of 40 mm

The effects noted above are dealt with in greater detail in the section that follows.

CORROSION RATES IN CRACKED CONCRETE – MAIN INFLUENCING FACTORS

a) Cracking and crack width

In the presence of cracks, concrete penetrability (the ease with which substances can penetrate into the concrete by any mechanism) may be significantly increased, especially when crack widths are sufficiently large. This results in increased corrosion rate and shorter service life of the RC structure. Figures 19 to 22 show that for a given concrete quality (binder type and w/b ratio), corrosion rate increases with increasing crack width (ranging from uncracked to 0.7 mm).

Figures 19 to 22 indicate that binder type and w/b ratio also have an important influence on corrosion rates. Table 10 shows mean corrosion rates (between weeks 26 to 31 when the rates were reasonably stable).

The data in Table 10 are also shown on Figure 18 (and as indicated, relate to weeks 26 to 31 of the measurements). The corrosion threshold of 0.1 μA/cm^2 is also indicated on Figure 18.

The following can be noted from Figure 18 and Table 10:

- All the uncracked and incipient-cracked specimens for all the binder types, except PC–55 uncracked, PC–40 and PC–55 incipient-cracked specimens, were still in the passive corrosion state i.e. $i_{corr} < 0.1$ μA/cm^2.
- All the 0.4 mm and 0.7 mm cracked specimens for all binder types exceeded the active corrosion threshold of 0.1 μA/cm^2.
- For the same w/b ratio, cracking has a greater impact on corrosion rates in plain PC concrete (resulting in at least a 210% increase) than in Corex slag concrete.

The influence of cracking and crack width on corrosion is further emphasised in Figures 23 to 25 where different crack widths are compared. The figures are plotted in terms of the 'centres of gravity' of the corrosion rate scatter points over the study period, for the different binder types. For clarity, the binder types are grouped within the oval shapes.

Clearly, corrosion rates for the cracked specimens for a given binder type are higher than those of uncracked specimens. Even incipient cracks have a large impact on corrosion rate compared to uncracked specimens. This contradicts the conventionally accepted theory that crack widths below 0.4 mm have no major impact on corrosion rate and shows that it is not possible to obtain a universal threshold crack width for all concretes.

Therefore, a threshold crack width may be applicable only for a specific concrete quality (binder type and w/b ratio) and/or concrete cover. The impact of crack width is less notable between the 0.4 and 0.7 mm cracked specimens (Figure 25) than between the uncracked and incipient-cracked specimens (Figure 23).

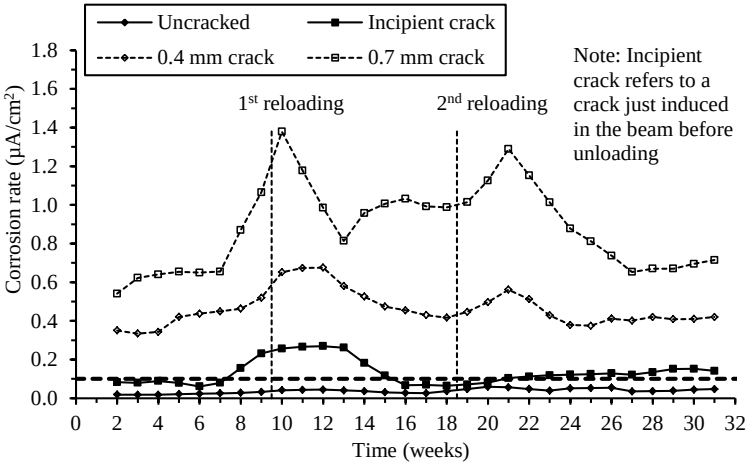

Figure 19: 3-point moving average corrosion rates - PC–40 mix (Otieno *et al.*, 2010b)

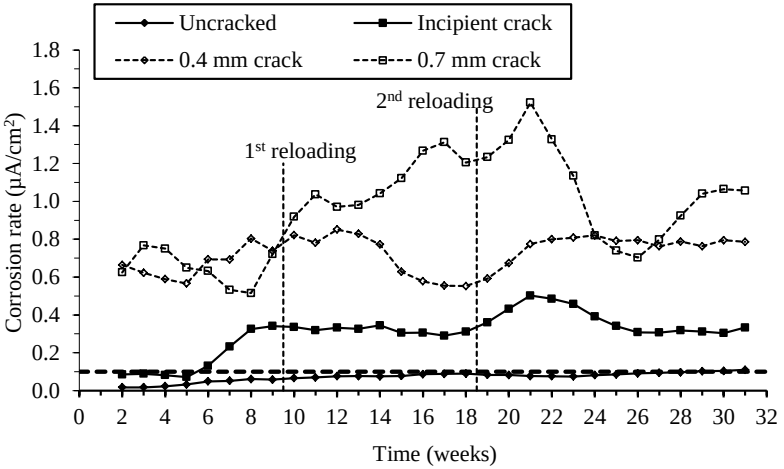

Figure 20: 3-point moving average corrosion rates - PC–55 mix (Otieno *et al.*, 2010b)

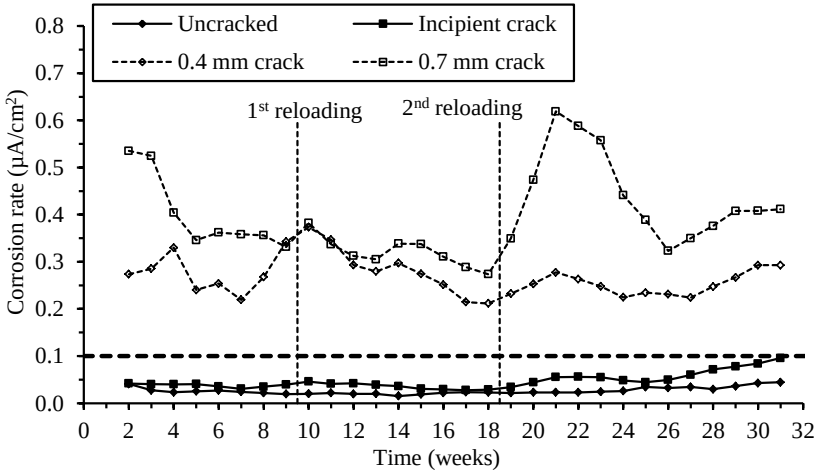

Figure 21: 3-point moving average corrosion rates - SL_C–40 mix (Otieno *et al.*, 2010b)

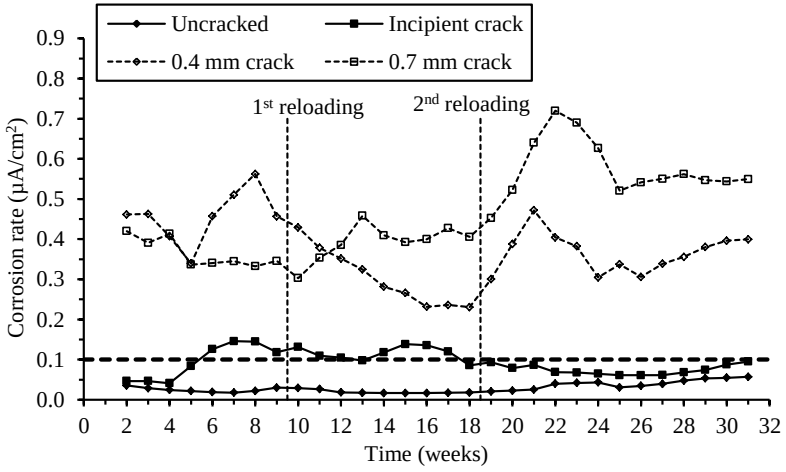

Figure 22: 3-point moving average corrosion rates - SL_C–55 mix (Otieno *et al.*, 2010b)

Table 10: Mean corrosion rates (week 26-31, µA/cm^2) (Otieno, 2008)

	PC–40	*PC–55*	*SL$_C$–40*	*SL$_C$–55*
Uncracked	**0.04**	0.10	**0.04**	**0.05**
Incipient-cracked	0.14	0.31	**0.07**	**0.07**
0.4 mm cracked	0.36	0.78	0.26	0.41
0.7 mm cracked	0.69	0.93	0.38	0.55

Legend - Corrosion: Passive; Moderate; High

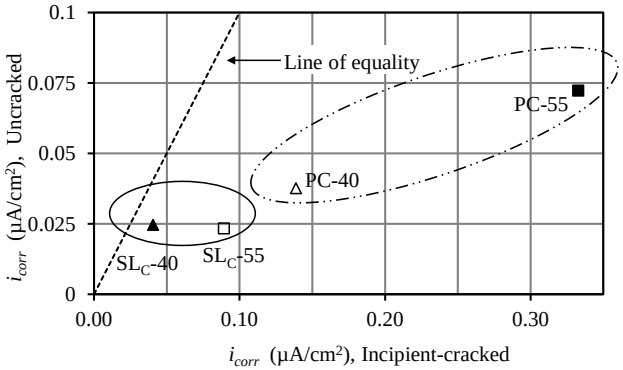

Figure 23: Comparison of corrosion rates for uncracked and incipient-cracked specimens (Otieno *et al.*, 2010a)

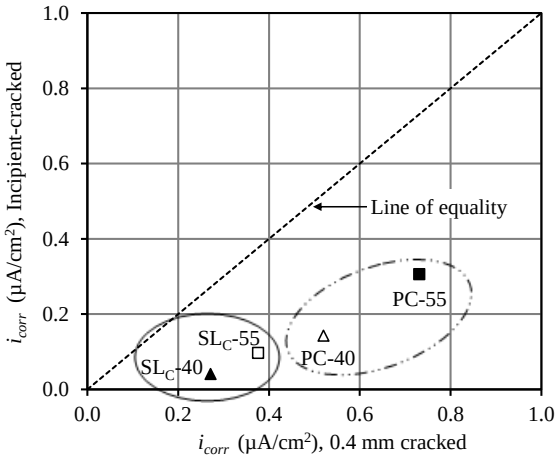

Figure 24: Comparison of corrosion rates for incipient-cracked and 0.4 mm cracked specimens (Otieno *et al.*, 2010a)

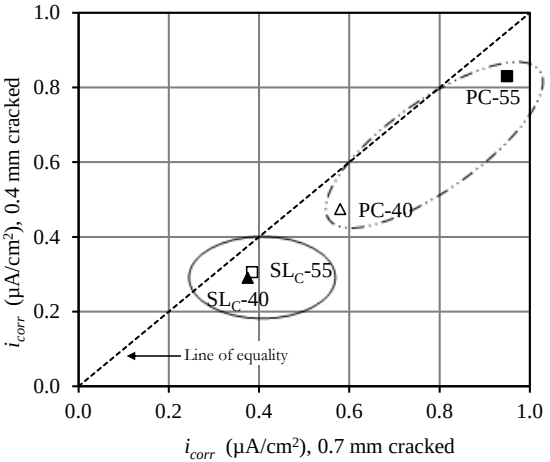

Figure 25: Comparison of corrosion rates for 0.4 and 0.7 mm cracked specimens (Otieno *et al.*, 2010a)

b) Concrete quality (binder type and w/b ratio)

With respect to corrosion, concrete quality is related to the combined effects of binder type and w/b ratio. These, in turn, have an important influence on the penetrability of the cover layer. Binder type has major influence on the chemistry of the system, while w/b ratio influences the pore structure.

Figures 19 to 22 show that for a given crack width, corrosion rates generally increased with decreasing concrete quality in the following order: SL_C–40 → SL_C–55 → PC–40 → PC–55. Corex slag specimens showed lower corrosion rates than plain PC specimens. As a general rule, blended cement concretes perform better, and often considerably better, than PC concretes with respect to corrosion.

c) Concrete resistivity

Concrete resistivity governs the ease with which current can flow through the concrete by ionic transport, in this case mainly OH^- ions. Both binder type and w/b ratio have an influence on the concrete resistivity. Low resistivity concretes offer less resistance to ionic movement, and therefore favour higher corrosion rates. Concrete resistivity is therefore an important factor when considering corrosion rates, especially for blended cement concretes.

Results such as those in Figure 26 indicate that blended cement concretes generally have high concrete resistivities, which can limit the corrosion rate. There is a large difference in the resistivities for plain Portland and Corex slag concretes. Regardless of the w/b ratio, PC concretes have lower resistivities than slag concretes.

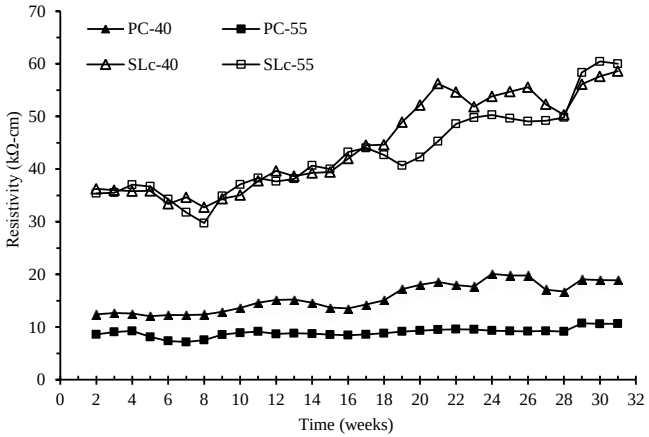

Figure 26: Moving average resistivity trends for both cracked and uncracked specimens (Otieno *et al.*, 2010a)

In concretes with high resistivity, the corrosion rate tends to be governed by this property - a condition termed 'resistivity control'. Blended cement concretes tend to exhibit higher resistivity and thus usually function under 'resistivity control' in regard to corrosion. This is illustrated in Figure 27, which shows that corrosion rates are inversely related to concrete resistivity. Corrosion rates for the slag specimens are lower than the corresponding PC specimens regardless of cracking.

Figure 27 also shows that concrete resistivity is more influential than crack width. For example, a 0.7 mm cracked SL_C–55 specimen had a lower corrosion rate than a 0.4 mm cracked PC–40 specimen. This shows the dominating nature of high concrete resistivity in controlling corrosion rate even in the presence of cracks, particularly for blended cement concretes. Thus, blended cements are very beneficial not only in extending the initiation period before corrosion commences but, just as importantly, in subsequently controlling corrosion rates in cracked concrete. *This implies that the propagation period can be considerably extended by the use of cement extenders.* Under these conditions, it may be possible to incorporate the

propagation period or a portion of it in the design life of the structure. In the case of cracked concrete members where, particularly in chloride conditions, the initiation period is minimal (as chlorides can readily reach the reinforcement), this observation is very important: it implies that the structure can remain serviceable even during the corrosion propagation phase, or a part of it.

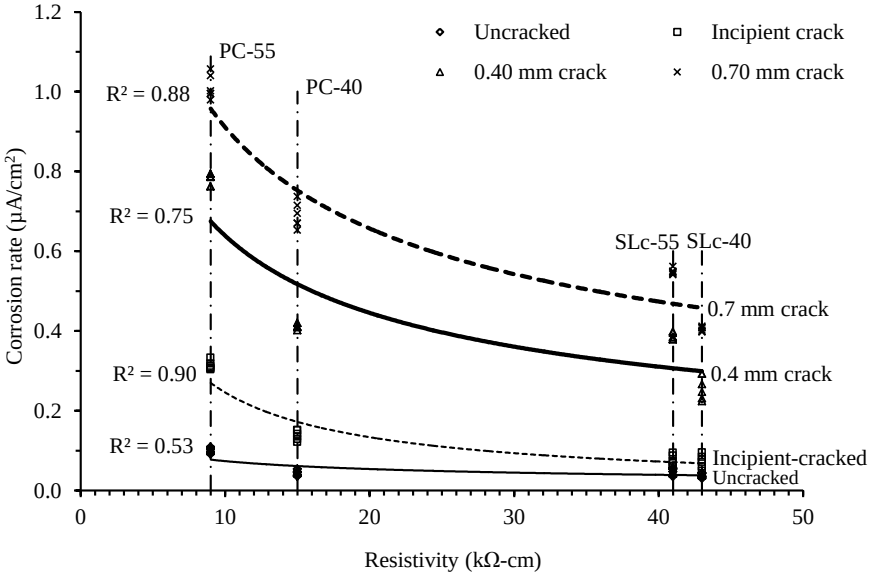

Figure 27: Relationship between average corrosion rate and concrete resistivity (weeks 26-31) (Otieno *et al.*, 2010b)

Figure 27 shows that for a given concrete quality (binder type and w/b ratio), corrosion rate increases with increasing crack width, but the resistivity of the cracked specimens remains unchanged i.e. for a given binder type there was no notable difference between the resistivity of uncracked and cracked specimens. This is true provided the measurements are taken in saturated or near-saturated concrete. Resistivity can therefore serve as a good first indicator for corrosion activity even in cracked RC structures.
A relationship also exists between the chloride conductivity index (CCI) and corrosion rate (Figure 28), but in this case it can be modelled as being linear which is an advantage.

Note the following on the use of resistivity to assess corrosion in cracked reinforced concrete structures:

(i) It should mainly be used as a first indicator of likely corrosion activity.

(ii) A means of also allowing for the effects of crack width is required, for example, using correction factors. These can only be determined using sufficient data from long-term studies.

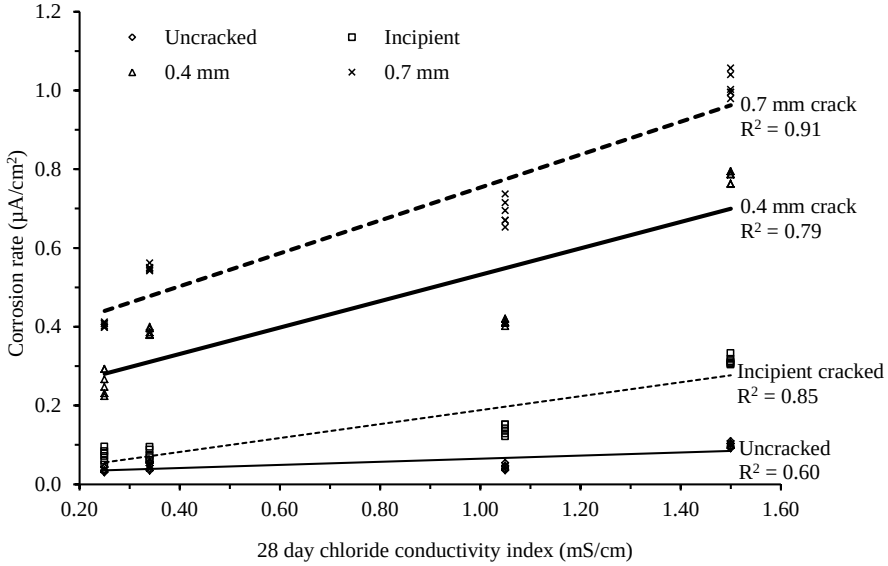

Figure 28: Relationship between 28 day CCI and average corrosion rate (weeks 26-31) (Otieno *et al.*, 2010b)

d) Concrete cover

Effect of cover on corrosion rates

Scott's work showed that the effect of cover on corrosion rate depends largely on the binder type. For plain Portland concretes, increased cover (in his case, from 20 mm to 40 mm) substantially reduced the corrosion rate for both 0.2 mm and 0.7 mm cracks widths – see Figure 29. By contrast, increasing the cover in the same range had little effect on the corrosion rate of concretes containing cement extenders.

The results can be explained by considering that oxygen is required for the corrosion reaction – specifically the cathodic reaction (see Equation 2). Increased cover reduces the availability of oxygen to the cathode by increasing the distance through which the oxygen must diffuse; it also delays drying at the depth of the steel.

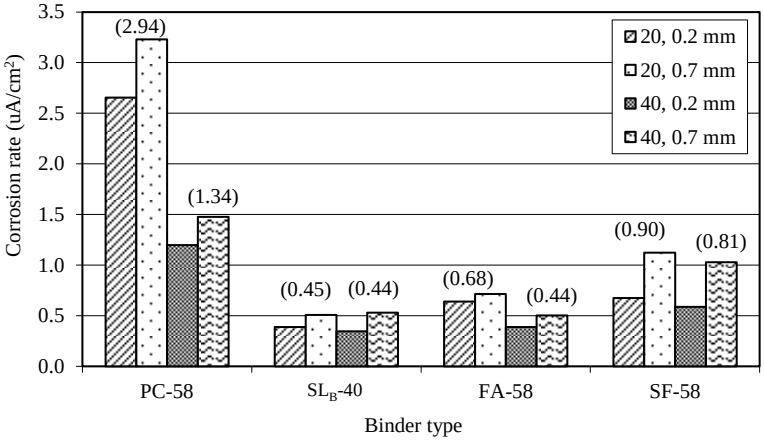

Figure 29: Effect of cover (20 mm or 40 mm) on corrosion rates (values in brackets above the bars are averages for the two crack widths for the relevant cover depths) (Scott, 2004)

The reason why plain Portland concretes are more susceptible to cover is, firstly because of their elevated corrosion rates which require more oxygen, and secondly because of their low resistivity which permits a higher corrosion rate. Concretes containing blended binders tend to have a sufficiently high resistivity so that an increase in cover has little effect.

These results lead to the postulate that *resistivity values in concrete with cement extenders tend to control the corrosion rate* - at least for covers up to about 40 mm (the maximum cover that Scott studied). As already discussed earlier, corrosion rates in these systems can be termed *'resistivity controlled'.*

Plain Portland concretes, however, do not have the controlling effect of high resistivity, and therefore *oxygen availability at the cathode is critical in controlling corrosion rates* - making them *'cathodically controlled'*. It is possible that at greater cover depths for blended cement concretes, a point might be reached where the availability of oxygen then controls the corrosion rate. (These principles are demonstrated later in Figure 30).

e) Crack re-opening or activation

The term *crack re-opening* refers to either widening of existing cracks or re-activating of self-healed ones by mechanical loading of the member. In either case, the process makes the crack active, and may be either cyclic or occasional. In the work of Otieno, two crack re-opening actions were

carried out. The first reloading (between weeks 9 and 10) was done to assess the influence of crack re-opening on the early corrosion rate (up to week 9) while the second reloading (between weeks 18 and 19) was done when corrosion rates had become reasonably stable, to evaluate whether crack re-opening may increase corrosion rate. Reloading was done by tightening the nuts in the loading rig (see Figure 31 in the Appendix) to open the 0.4 mm, 0.7 mm and incipient cracks to 0.6 mm, 1.0 mm and 0.2 mm respectively. The reloading crack widths were selected based on the maximum crack width to which the 0.7 mm crack could be opened without yielding of the steel. The crack widths at reloading were maintained for about 24 h before being relaxed to their original respective widths.

The effects of crack re-opening can be summarized as follows, based on information given in Figure 19 to 22:

- Crack re-opening increases corrosion rate *but only if the RC structure was actively corroding prior to crack re-opening* (i.e. corrosion rate was greater than 0.1 $\mu A/cm^2$).
- For passively corroding RC members, the effect of reloading may allow chlorides to reach the embedded steel and start (or accelerate) the destruction of the passive protective layer.
- If cracks are subsequently allowed to remain dormant, corrosion rates reduce again, which infers some form of crack-healing.

For an actively corroding RC structure, crack re-opening may accelerate the corrosion process by one or a combination of the following mechanisms: a) widening the existing cracks, b) re-activating (re-opening) any self-healed cracks, c) increasing the loading level (i.e. stressing the steel), and d) damaging the concrete-steel and/or aggregate-paste interfaces.
Table 11 gives the percentage increases in corrosion rates after a crack re-opening process, taken from the data in Figure 19 to Figure 22.

Table 11: Percentage increases in corrosion rates after crack re-opening (Otieno, 2008)

	Percentage increase in i_{corr} after crack re-opening (%)			
Specimen condition	*PC – 40*	*PC – 55*	*SL_C – 40*	*SL_C – 55*
Incipient-cracked	3	16	8	9
0.4 mm cracked	13	7	10	30
0.7 mm cracked	11	2	28	12

In general, incipient-cracked (except PC–55) specimens experienced the lowest percentage increases in corrosion rate due to crack re-opening, while the 0.4 mm and 0.7 mm cracked specimens showed a higher increase. Note also:

- The 0.4 mm cracked specimens were actively corroding before the crack re-opening process.
- For all binder types (except PC–55), the incipient-cracked specimens were passive (corrosion rate below 0.1 $\mu A/cm^2$) before and after the crack re-opening, a condition which did not favour corrosion rate increasing substantially. Crack self-healing probably occurred in these specimens although this was not measured. Further studies are required to quantify this phenomenon.

The minimal 2% increase in corrosion rate for the 0.7 mm cracked PC–55 specimens (which were actively corroding before the reloading process) means that even before reloading, corrosion agents could easily penetrate to the steel and promote corrosion. Crack re-opening therefore did not affect the concrete penetrability to a great extent, with respect to corrosion rate, in these specimens.

DISCUSSION

The presence of cracks, crack re-opening or crack re-activation, low cover, and lower concrete quality all increase corrosion rates of RC members in chloride environments. In Otieno's study, cracks (even 'incipient' cracks) increased corrosion rate by at least 40% and 210% in the blended and plain cement concretes respectively in comparison with uncracked concrete. Corrosion rate increased with increase in crack width and decrease in concrete quality (increase in w/b ratio). Scott showed the influence of cover which was substantial only in the case of plain Portland concretes.

While blended cement concrete (SL_B–58, SL_C–55, SL_C–40, FA–58, SF–58 and TR–58) is adversely affected by cracking, this is much less so than plain Portland cement concrete. *This reinforces the imperative of using blended cements rather than plain cements for concrete in marine environments*. The high concrete resistivity in blended cement concretes governs the corrosion rate in these concretes and consequently diminishes the effects of cracking. The corrosion process in blended cement concretes is more resistivity-controlled than cathodically-controlled. Corex slag concretes are also less sensitive to changes in w/b ratio (from 0.4 to 0.55). This finding is advantageous for situations where strict construction su-

pervision is not in place and where human error is more likely to be encountered.

The results of this study contradict the general notion that crack widths less than 0.4 mm do not significantly affect steel corrosion in RC structures. This work showed that crack widths below 0.4 mm (e.g. incipient cracks) may significantly affect both the initiation and propagation of corrosion depending on the concrete quality and type. The 0.4 mm threshold crack width did not apply even in the slag specimens (see Figure 18). It is therefore not possible to set a *universal threshold crack width* for all concrete types (binder type and w/b ratio) and/or cover.

Crack re-opening or re-activation affects the corrosion process depending on whether the RC structure is in an active or passive corrosion state prior to reloading. For actively corroding structures, reloading tends to increase corrosion rate; for passively corroding structures, reloading serves to increase chloride ingress and start (or accelerate) the destruction of the passive protective layer (although the latter was not investigated).

GENERAL CONCLUSIONS

The studies discussed in this monograph have contributed to an improved understanding of the combined influences of cracking, crack width, crack re-opening, cover depth, binder type and w/b ratio on chloride-induced corrosion in RC members. The following general conclusions can be drawn:

(i) Cracks accelerate chloride-induced corrosion by increasing concrete penetrability. The wider the crack, the higher the corrosion rate. However, the effect of cracks on corrosion rate is modified by concrete quality.

(ii) In general, improved concrete quality (represented by binder type and w/b ratio) may be used to help control corrosion in cracked (and uncracked) concrete, specifically for slag blended concretes.

(iii) Blended cement concretes, where corrosion rate tends to be governed by the high concrete resistivity, are less sensitive to the effects of cracking compared to plain Portland cement concretes with low resistivity. Blended cement concretes are also considerably less sensitive to changes in w/b ratio than PC concretes.

(iv) Increasing cover depth has a substantial benefit for PC concretes but the same benefits of increased cover are not observed in blended cement concretes (slag, fly ash and silica fume) where reduced corrosion rates in comparison with PC are noticeable even without increas-

ing cover owing to lower permeability and higher resistivity. The use of supplementary cementitious materials (slag, fly ash and silica fume) is more effective in controlling corrosion in cracked and uncracked concrete than increasing the cover depth.

(v) It is not possible to obtain a *universal threshold crack width* for all concretes below which corrosion is similar to uncracked concrete.

(vi) Reloading of corroding RC structures accelerates corrosion by one or a combination of the following: re-activating or re-opening self-healed cracks, widening the existing ones, increasing the loading level (i.e. stress in the steel), and damaging the concrete-steel and/or aggregate-paste interfaces. However, the effect of reloading is more significant if the RC structure was actively corroding prior to reloading.

DESIGN IMPLICATIONS

Regardless of the concrete quality (binder type and w/b ratio), cracks increase corrosion rate of RC members in chloride conditions. However, the resulting corrosion rate will depend not only on the crack width, but also on the concrete quality and cover to steel.

A fundamental difference exists between plain Portland cement concretes and slag-blended concretes. In plain concretes, resistivity is usually relatively low which means that the ionic flow required for the corrosion reaction is largely unimpeded. Thus, resistivity is usually not a controlling factor in corrosion propagation. By contrast, blended cement concretes generally have relatively high resistivity which then becomes the main controlling factor in the corrosion rate; for corrosion propagation, cover to steel is a secondary factor in such systems (however, note that cover is still a very important factor for corrosion initiation).

For plain concretes, the corrosion controlling parameter tends to be oxygen availability at the cathode; such systems are termed ‘cathodically controlled’. The ease with which oxygen can permeate to the steel is therefore a crucial factor. Consequently cover depth is more critical in plain concretes in order to control corrosion. These concepts are illustrated in Figure 30. Figure 30 gives a general example of the interaction between corrosion rate, resistivity and availability of oxygen.

Figure 30 (a): In this figure, the availability of oxygen at a given cover depth is defined by curve ACE (compare the curves in Figure 14). The same curve is also used as a representation of the corrosion rate even if

there is sufficient oxygen to support a higher reaction rate. The resistivity controls are shown as horizontal lines 'PC Resistivity' and 'SCM Resistivity', where PC would be representative of plain PC concretes, and SCM of concretes produced with slags (or other blended cements)[1].

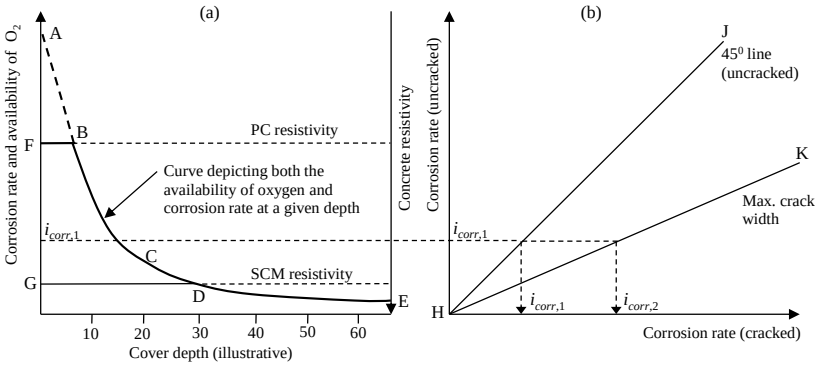

Figure 30: Schematic of the relationship between corrosion rate, O_2 availability, resistivity and crack width (PC: plain Portland cement, SCM: supplementary cementitious materials) (Otieno, 2008).

Consider a specimen with a resistivity given by 'PC'. The possible corrosion rate curve is given by the composite line FBCE. It is clear that the corrosion rate (on the left hand axis of Figure 30 (a)) is very sensitive to cover depth, particularly for low cover. These rates are oxygen-availability dependent. Conversely, for a slag concrete (resistivity 'SCM'), the corrosion rate curve is given by the line GDE. Corrosion rate is now relatively insensitive to cover depth, and will be mainly resistivity-controlled (although obviously cover depth will exercise a secondary influence)[2].

[1] The horizontal lines should more properly be thought of as conductivity lines, where conductivity is the inverse of resistivity; also, the lines would likely be sloped somewhat to account for the variation in resistivity with cover depth. More research would be required to define the slopes of these lines, but for the purposes of the current discussion a horizontal line is sufficient.

[2] In the work reported here, no direct measurements of oxygen were made at the depth of the steel, and the proposal of the limiting effect of oxygen is based on a synthesis of the measured corrosion rates, resistivity values, the fact that the cathodic process is based on the reduction of oxygen, and available literature.

Figure 30 (b): This part of the figure illustrates how crack width can be accounted for. For design purposes, the maximum crack width (represented by line HK in Figure 30 (b)) should be set to the crack width that is tolerable with respect to corrosion, taking into consideration both the cover depth and concrete quality. Other factors such as crack self-healing can also be considered, depending on whether they increase or decrease corrosion rate. Corrosion rates for crack widths between zero (uncracked) and the maximum crack width can then be obtained by interpolation using sound engineering judgment.

In summary:

(i) For reinforcement corrosion control in chloride environments, the factors of crack width, crack re-opening (i.e. load variation) and concrete quality (binder type and w/b ratio) must be quantified and taken into consideration. Further research is needed to address this.

(ii) Service life models can also be modified to account for these factors and hence provide more accurate service life prediction.

(iii) However, further studies are still required to achieve this level of detailed design approach due to the numerous variables and uncertainties involved. This also means that we have to account for the stochastic nature of corrosion and corrosion induced cracking, and its spatial and temporal variation. This will doubtless follow in due course. In the meantime, this monograph should be useful in providing a framework that can be improved for practical applications.

CLOSURE

This monograph has dealt with corrosion of steel in reinforced concrete, whether cracked or uncracked, with the focus on chloride environments. The problem of steel corrosion in RC structures in service remains one of the foremost durability challenges for structural concrete engineers and researchers.

In Part I, the fundamentals of steel corrosion in concrete were comprehensively covered. The electro-chemical nature of corrosion was emphasized and important influencing parameters such as binder type and content, water/binder ratio, concrete resistivity, cover thickness, and cracking were dealt with. The stages of corrosion, generally described as the initiation phase and the propagation phase, were described. Corrosion measurement techniques were also briefly reviewed.

In Part II, recent research work at UCT was reviewed and summarised with a view to improving our understanding of the basic phenomena and

practical approaches to addressing the problems. The experimental studies comprised, firstly, aqueous phase work to examine the influence of different binder compositions and, secondly, actual corrosion measurements on cracked and uncracked RC beam specimens. Cracking was shown to have a dominant influence on the initiation phase and an important influence on the propagation phase. An important distinction needs to be drawn between plain Portland cement concretes on the one hand, and blended cement concretes on the other, in respect of corrosion. In the case of the former, cover depth is of critical importance since corrosion is largely controlled by the cathodic reaction, which translates into the ability of oxygen to penetrate through the cover layer - hence the importance of its thickness. For blended cement concretes, the concrete resistivity tends to be the governing parameter, with cover depth being less critical although not unimportant.

The experimental studies show conclusively that not only do blended cement concretes have extended initiation periods in comparison with plain concretes, all else being equal, but they also experience significantly lower corrosion rates during the propagation phase. From a design perspective, the monograph can assist engineers in making better decisions around binder type and cover depth for a given crack width arising from the design requirements. Using this information, designers can better manage reinforced concrete structures that are cracked in service and exposed to chloride environments, so as to have extended useful working lives.

REFERENCES

ACI-Committee-224R-01 (2001) Control of cracking in concrete structures. *American Concrete Institute*.

ACI-Committee-365 (2005) Service life prediction. *Report No. ACI 365.1R*, 38800 Country Club Drive, Farmington Hills, MI 48331 U.S.

Alexander, M. G., Ballim, Y. & Mackechnie, J. R. (2001) Use of durability indexes to achieve durable cover concrete in reinforced concrete structures. *Materials Science of Concrete,* VI, pp. 483-511.

Alexander, M. G. & Beushausen, H. (2007) Performance-based durability design and specification in South Africa. *Proceedings of the International Concrete Conference and Exhibition (ICCX - Concrete Awareness)*, 14-16 February, 2007, Cape Town, South Africa.

Alonso, C., Andrade, C., Rodriguez, J. & Diez, J. M. (1998) Factors controlling cracking of concrete affected by reinforcement corrosion. *Materials and Structures,* Vol. 31, pp. 435-441.

Andrade, C. & Alonso, C. (1996) Corrosion rate monitoring in the laboratory and on-site. *Construction and Building Materials,* Vol. 10(5), pp. 315-328.

Andrade, C., Alonso, C. & Molina, F. J. (1993) Cover cracking as a function of bar corrosion: Part I-Experimental test. *Materials and Structures,* Vol. 26, pp. 453-464.

Arya, C., Buenfeld, N. R. & Newman, J. B. (1990) Factors influencing chloride binding in concrete. *Cement and Concrete Research* Vol. 20, pp. 291-300.

Arya, C. & Ofori-Darko, F. K. (1996) Influence of crack frequency on reinforcement corrosion in concrete. *Cement and Concrete Research,* Vol. 26(3), pp. 333-353.

Arya, C. & Wood, L. (1995) The relevance of cracking in concrete to corrosion of reinforcement. *Concrete Society*. Technical report No. 44.

ASTM-C876-91 (1999) *Standard test method for half-cell potentials of uncoated reinforcing steel in concrete*, ASTM International, West Conshohocken, PA.

Ballim, Y. (1993) Towards an early age index for the durability of concrete. *Proceedings of international conference, Concrete 2000 - Economic and durable construction through excellence*. 7-9 September, 1993, Dundee, Scotland, Volume 2, E & FN Spon, London. pp. 1003-1012.

Beeby, A. (1983) Cracking, cover and corrosion of reinforcement. *Concrete International,* Vol. 5(2), pp. 35-40.

Bentur, A., Diamond, S. & Berke, N. (1997) *Steel corrosion in concrete, Fundamentals and Civil Engineering Practice*, E & FN Spon, London. pp. 41-43.

Bockris, J., Conway, B., Yeager, E. & White, R. Ed. (1981) *Comprehensive treatise of electrochemistry, Electrochemical Materials Science*, Vol. 4. Plenum Press, New York.

Boddy, A., Bentz, E., Thomas, M. D. A. & Hooton, R. D. (1999) An overview and sensitivity study of a multi-mechanistic chloride transport model. *Cement and Concrete Research,* Vol. 29**,** pp. 827-837.

Broomfield, J. P. (2007) *Corrosion of steel in concrete - understanding, investigation and repair (2nd Edition)*, Taylor & Francis, Oxford, United Kingdom.

BS-EN-206-1 (2000) *Concrete - Part 1: Specification, performance, production and conformity*, European Standard.

BS-EN-1992-1-1 (2004) Eurocode 2: Design of concrete structures - Part 1-1: General rules and rules for buildings. European Standard.

Dhir, R. K., El-Mohr, M. A. K. & Dyer, T. D. (1996) Chloride binding in GGBS concrete. *Cement and Concrete Research,* Vol. 26**,** pp. 1767-1773.

DuraCrete (1998) Probabilistic performance-based durability design: modelling of degradation. Document, D. P. No. BE95-1347/R4-5, The Netherlands.

Edvardsen, C. (1999) Water permeability and autogenous healing of cracks in concrete. *ACI Materials Journal,* Vol. 96(4)**,** pp. 448-454.

El Maaddawy, T. & Soudki, K. (2007) A model for prediction of time from corrosion initiation to corrosion cracking. *Cement & Concrete Composites,* Vol. 29(3)**,** pp. 168-175.

fib-Model-Code (2010) 3rd FIP/CEB Model Code for concrete structures. *Comite Euro-International du Beton and Federation International de Precontrainte*.

Glass, G., Page, C., Short, N. & Yu, S. (1993) An investigation of galvanostatic transient methods used to monitor the corrosion rate of steel in concrete. *Corrosion Science,* Vol. 35(No. 5-8)**,** pp. 1585-1592.

Gouda, V. K. & Halaka, W. Y. (1970) Corrosion and corrosion inhibition of reinforcing steel embedded in concrete. *British Corrosion Journal,* Vol. 5**,** pp. 204-208.

Hassanien, A., Glass, G. & Buenfeld, N. (1998) The use of small electrochemical perturbations to assess the corrosion of steel in concrete. *NDT&E International,* Vol. 31(4)**,** pp. 265–272.

Heckroodt, R. O. (2002) *Guide to deterioration and failure of building materials*, Thomas Telford Ltd, 1 Heron Quay, London E14 4JD.

Hunkeler, F. (2005) *Corrosion in reinforced concrete structures*, Woodhead publishing limited, Abington Hall, Abington Cambridge CBI 6AH, England. pp. 1-45.

JSCE (1986) Standard Specification for Design and Construction of Concrete Structures - Part 1 (Design). *Japan Society of Civil Engineers*, SP-1, Tokyo, Japan.

Li, M. & Li, V. C. (2011) Cracking and healing of engineered cementitious composites under chloride environment. *ACI Materials Journal,* Vol. 108(3)**,** pp. 333-340.

LIFE-365 (2005) ACI-Committee-365, Service life prediction model, Computer program for predicting the service life and life-cycle costs of reinforced concrete exposed to chlorides. *American Concrete Institute*.

Liu, T. & Weyers, R. W. (1998) Modelling the dynamic corrosion process in chloride contaminated concrete structures. *Cement and Concrete Research,* Vol. 28(3)**,** pp. 365-379.

Liu, Y. (1996) Modelling the time-to-corrosion cracking of the cover concrete in chloride-contaminated reinforced concrete structures. *PhD Thesis,* Department of civil engineering, Virginia Polytechnic Institute and State University.

Luo, R., Cai, Y., Wang, C. & Huang, X. (2003) Study of chloride binding and diffusion in GGBS concrete. *Cement and Concrete Research,* Vol. 33**,** pp. 1-7.

Mackechnie, J. & Alexander, M. G. (1996) Marine exposure of concrete under selected South African conditions. *Third ACI/CANMET Int. Conference on the Performance of Concrete in Marine Environment*. St. Andrews, Canada. pp. 205-216.

Mackechnie, J. R. (1996) Predictions of reinforced concrete durability in the marine environment. *PhD Thesis,* Department of civil engineering, University of Cape Town.

Mackechnie, J. R. (1997) Predictions of reinforced concrete durability in the marine environment. *Research Monograph No. 1,* University of Cape Town and the University of Witwatersrand.

Mackechnie, J. R. & Alexander, M. G. (2001) Repair principles for corrosion-damaged reinforced concrete structures. *Research Monograph No. 5,* University of Cape Town and the University of Witwatersrand.

Mackechnie, J. R., Alexander, M. G. & Jaufeerally, H. (2003) Structural and durability properties of concrete made with Corex slag, *Research monograph No. 6,* Department of civil engineering, University of Cape Town.

Mackechnie, J. R., Alexander, M. G., Heiyantunduwa, R. & Rylands, T. (2004) The effectiveness of organic corrosion inhibitors for reinforced concrete. *Research Monograph No. 7,* University of Cape Town and the University of Witwatersrand.

Manera, M., Vennesland, O. & Bertolini, L. (2008) Chloride threshold for rebar corrosion in concrete with addition of Silica Fume. *Corrosion Science,* Vol. 50(2)**,** pp. 554-560.

Mangat, P. S., El-Khatib, J. M. & Molloy, B. T. (1994) Microstructure, chloride diffusion and reinforcement corrosion in blended cement paste and concrete. *Cement and Concrete Composites,* Vol. 16(2)**,** pp. 73-81.

Molina, F. J., Alonso, C. & Andrade, C. (1993) Cover cracking as a function of rebar corrosion: Part II-Numerical model. *Materials and Structures,* Vol. 26**,** pp. 532-548.

Neville, A. M. (2002) Autogenous healing - a concrete miracle? *Concrete International,* Vol. 24(11)**,** pp. 76-82.

Oh, B. H., Jang, S. & Shin, Y. S. (2003) Experimental investigation of the threshold chloride concentration for corrosion initiation in reinforced concrete structures. *Magazine of Concrete Research,* Vol. 55**,** pp. 117-124.

Otieno, M. B. (2008) Corrosion propagation in cracked and uncracked concrete. *Masters Dissertation*, Department of civil engineering, University of Cape Town.

Otieno, M. B., Alexander, M. G. & Beushausen, H.-D. (2010a) Corrosion in cracked and uncracked concrete - influence of crack width, concrete quality and crack re-opening. *Magazine of Concrete Research,* Vol. 62(6)**,** pp. 393-404.

Otieno, M. B., Alexander, M. G. & Beushausen, H.-D. (2010b) Suitability of various measurement techniques for assessing corrosion in cracked concrete. *ACI Materials Journal,* Vol. 107(5)**,** pp. 481-489.

Pal, S. C., Mukherjee, A. & Pathak, S. R. (2002) Corrosion behaviour of reinforcement in slag concrete. *ACI Materials Journal,* Vol. 99(6)**,** pp. 1-7.

Parrot, L. J. (1987) A review of carbonation in reinforced concrete. *Cement and Concrete Association,* United Kingdom, Wexham Springs, Slough.**,** pp. 257-266.

Pettersson, K. (1995) Chloride threshold value and the corrosion rate in reinforced concrete. *Proceedings of Nordic Seminar*. Lund.

Pettersson, K. & Jorgensen, O. (1996) The effect of cracks on reinforcement corrosion in high-performance concrete in a marine environment. *Third ACI/CANMET Int. conference on the Performance of Concrete in Marine Environment*. St. Andrews, Canada. pp. 185-200.

Richardson, M. G. (2002) *Fundamentals of durable concrete*, Modern Concrete Technology, Spon Press, London.

RILEM_TC154-EMC (2004) Electrochemical techniques for measuring metallic corrosion - recommendations - test methods for on-site corrosion rate measurement of steel reinforcement in concrete by means of the polarization resistance method. *Materials and Structures,* Vol. 37**,** pp. 623-643.

Rodriguez, P. & Gonzalez, J. (1994) Use of the coulostatic method for measuring corrosion rates of embedded metal in concrete. *Magazine of Concrete Research,* Vol. 45(167)**,** pp. 91-97.

Schießl, P. & Edvardsen, C. (1993) Autogenous healing of cracks in concrete structures subjected to water pressure. *Report No. F361***,** Institute of Building Materials Research, RWTH Aachen University.

Schießl, P. & Raupach, M. (1997) Laboratory studies and calculations on the influence of crack width on chloride-induced corrosion of steel in concrete. *ACI Materials Journal,* Vol. 94(1)**,** pp. 56-62.

Scott, A. N. (2004) The influence of binder type and cracking on reinforcing steel corrosion in concrete. *PhD Thesis*, Department of civil engineering, University of Cape Town.

Scott, A. N. & Alexander, M. G. (2007) The influence of binder type, cracking and cover on corrosion rates of steel in chloride-contaminated concrete. *Magazine of Concrete Research,* Vol. 59(7)**,** pp. 495-505.

Shreir, L. L., Jarman, R. A. & Burstein, G. T. (Editors) (1994) *Corrosion - Metal/Environment reactions*, 3rd Edition (Volume 1)**,** Published by Butterworth-Heinemann, Linacre House, Jordan Hill, Oxford X2 8DP, 225 Wildwood Avenue, Woburn, MA 01801-2041, p. 17.

Stern, M. & Geary, A. L. (1957) Electrochemical polarization - I: theoretical analysis of shape of polarization curves. *Journal of Electrochemistry Society*, Vol. 104**,** pp. 56-63.

Suzuki, K., Ohno, Y., Praparntanatorn, S. & Tamura, H. (1990) *Mechanism of steel corrosion in cracked concrete*. Page, C., Treadaway, K. & Bramforth, P. Corrosion of reinforcement in concrete. London: Society of Chemical Industry**,** pp. 19-28.

Tang, L. (1996) Chloride transport in concrete – measurement and prediction. *PhD Thesis*, Chalmers University of Technology, Gotenburg, Sweden.

Tarek, U. M., Yamaji, T. & Hamada, H. (2002) Chloride diffusion, microstructure and mineralogy of concrete after 15 years of exposure in tidal environment. *ACI Materials Journal*, Vol. 99(3)**,** pp. 256-263.

Thomas, M. (1996) Chloride threshold in marine concrete. *Cement and Concrete Research*, Vol. 26**,** pp. 513-519.

Zivica, V. (2003) Influence of w/c ratio on rate of chloride induced corrosion of steel reinforcement and its dependence on ambient temperature. *Bulletin of Materials Science*, Vol. 26(5)**,** pp. 471-475.

APPENDIX: EXPERIMENTAL DETAILS FOR SCOTT AND OTIENO

SCOTT'S EXPERIMENTAL DETAILS

Corrosion rates were measured on concrete specimens with crack widths of approximately 0.2 mm and 0.7 mm and cover depths of 20 mm and 40 mm. Five binder combinations in specimens with 40 mm cover were studied, comprising plain Portland Cement (PC) (CEM I 42.5N), and PC blends with various replacements of extenders as follows: GGBS at 50% (SL_B–58); fly ash at 30% (FA–58); condensed silica fume at 7% (SF–58); and a ternary blend of 50% PC, 43% GGBS and 7% SF (TR–58). Four binder combinations of PC, SM, FA and SF were examined for 20 mm cover specimens. Constant water:binder ratio (w/b) of 0.58 was used for all concrete mixtures. The oxide and mineralogical analyses of the binders used are presented in Table 12 and the mix proportions and 28 day strengths for the concretes are given in Table 13.

Smooth mild steel round bars of 16 mm diameter were cast into concrete specimens (375 x 120 x 120 mm prisms) at cover depths of 20 mm or 40 mm. The bars were brushed to remove mill scale and thoroughly cleaned. A wire was attached to one end and both ends were heat shrink-wrapped and epoxy-coated to provide an exposed surface area of approximately 158 cm^2. Prior to casting, the bars were again cleaned and degreased with acetone.

The specimens were demoulded after 24 hours and water-cured until day 14 at 23 ^oC, whereafter a centrally located transverse crack was created in the specimens by three-point bending. There was some relaxation of the crack once the load was removed and thus it was necessary to initially provide a somewhat higher load to the specimen. The crack widths were measured and those corresponding to surface widths of approximately 0.2 mm and 0.7 mm were chosen. The cracks were induced and maintained through partial slipping of the round bar (Pettersson and Jorgensen, 1996). A reservoir was created on the surface and specimens exposed to a weekly cycle of three days wetting with a 5% NaCl solution and four days drying at 30 ^oC. A number of identical uncracked specimens, with 20 mm cover, were also cast and subjected to the same exposure conditions for comparative purposes.

Three specimens for each combination of binder type, cover depth and crack width were monitored bi-weekly for corrosion potential and rate, and concrete resistivity. The three individual specimen readings were then averaged to provide one result. Resistivity was measured using a 4 probe Wenner instrument. Potential was monitored against a Ag/AgCl reference electrode. Corrosion rate data were obtained by means of a coulostatic technique whereby a small charge was applied to the steel and the relaxation of potential was monitored over a short period of time, typically one minute, to determine the polarization resistance R_P. The theoretical development and principles of the coulostatic method have been presented in a number of sources (Glass *et al.*, 1993, Hassanien *et al.*, 1998, Scott and Alexander, 2007). The polarization resistance was converted into a corrosion rate (i_{corr}) by means of the Stern-Geary relationship given in Equation 13 (Rodriguez and Gonzalez, 1994), with an assumed constant value B of 26 as suggested by Andrade and Alonso (1996).

$$i_{corr} = \frac{B}{R_p} \tag{13}$$

Table 12: Analyses of binder materials (%)

Oxide	*PC*	*GGBS*	*FA*	*SF*	*Mineralogy* (PC)*	*%*
SiO_2	21.5	35.7	53.1	91.9	C_3S	65.5
CaO	65.9	34.3	4.2	0.0	C_2S	12.3
Al_2O_3	3.7	13.6	33.7	0.7	C_3A	3.72
Fe_2O_3	3.6	0.7	3.6	0.8	C_4AF	10.94
Mn_2O_3	0.06	1.10	0.05	0.09	* By Bogue Formulae	
TiO_2	0.18	0.60	1.77	0.11		
MgO	0.88	10.20	1.02	0.26		
SO_3	3.28	2.86	0.30	0.46		
K_2O	0.54	0.80	0.75	1.33		
Na_2O	0.19	0.20	0.40	0.42		

Table 13: Concrete mix proportions (all units in kg/m^3, except Superplasticizer*(S.P.) in Litres) and 28 day strengths (MPa)

Material	*PC–58*	*SL_B–58 (50%)*	*FA–58 (30%)*	*SF–58 (7%)*	*TR–58 (50:43:7)*
Water	175	175	175	175	175
CEM I 42.5N (PC)	302	151	211	281	151
GGBS	-	151	-	-	130
Fly ash (FA)	-	-	91	-	-
Silica fume (SF)	-	-	-	21	21
Sand	750	750	750	750	750
Stone (9 mm)	1050	1050	1050	1050	1050
w/b ratio	0.58	0.58	0.58	0.58	0.58
28 day compressive strength	46.5	42.7	42.2	49.7	46.5
S.P. (Sika 163) (L)	-	-	-	1.5	1.5

OTIENO'S EXPERIMENTAL DETAILS

Corrosion rates were measured on both uncracked and cracked (incipient crack, 0.4 mm and 0.7 mm crack width) 100 x 100 x 500 mm concrete specimens with a cover depth of 40 mm. Four concrete mixes were made using two w/b ratios (0.40 and 0.55) and two binder types (100% CEM I 42.5N (PC), and 50/50 PC/Corex slag blend). The mix proportions and 28 day strengths for the concretes used are presented in Table 14.

Table 14: Concrete mix proportions (all units in kg/m^3, except 28 day strengths (MPa))

	100 % PC		*50/50 PC/GGCS*	
Material	*PC–40*	*PC–55*	*SL_C–40*	*SL_C–55*
PC (CEM I 42.5N)	463	336	231	168
Corex slag	-	-	231	168
Sand	749	855	749	855
Stone (19 mm)	1040	1040	1040	1040
Water content	185	185	185	185
w/b ratio	0.40	0.55	0.40	0.55
28 day compressive strength	49.5	32.5	51.9	33.0

For each binder type, crack width and w/b ratio, three specimens were cast, hence there was a total of 48 specimens. Ground granulated Corex slag (GGCS) is a cementitious material produced during the Corex process for iron production; it has similar characteristics to ground granulated

blastfurnace slag (Mackechnie *et al.*, 2003). Crushed greywacke stone (max. size 19 mm) and dune sand were used as aggregate.

High yield 10 mm diameter deformed steel reinforcement bars ($f_y \approx 550$ MPa) were used, with a clear concrete cover of 40 mm. Prior to casting, the bars were wire-brushed to remove mill scale. A wire was attached to one end of the bars and both ends were epoxy-coated to provide an exposed surface area of approximately 94 cm^2. Immediately before casting, the bars were de-greased with acetone. A 10 mm diameter x 100 mm long stainless steel bar was placed in each concrete beam during casting (Figure 31) to act as a counter electrode for corrosion rate measurements using the coulostatic technique (Stern and Geary, 1957, Hassanien *et al.*, 1998).

During casting, 1.0 mm thick x 10 mm deep PVC sheets were placed (perpendicular to the beam longitudinal axis) at the centre of each beam to induce cracks at the centre of the specimens during pre-cracking. After 28 days of water curing (at 23 ± 2 ^oC) and 10 days air drying, the beams were pre-cracked under 3-point flexural machine loading. The incipient cracks were produced by loading until a crack was visually detected using a hand-held lens, and then unloading after which the crack was no longer visible. The 0.4 and 0.7 mm crack widths were measured using a crack width detection microscope with a magnification and accuracy of X40 and 0.02 mm respectively, and were maintained using the loading rig shown in Figures 31 and 32. All the 0.4 and 0.7 mm cracked specimens remained in individual loading rigs for the duration of the experimental programme.

The specimens were subjected to a weekly cycle of 3 days ponding with 5% NaCl solution followed by 4 days air drying. To monitor the constancy of the crack widths, Demec studs were placed on the concrete surface across the crack. The distance between the studs was monitored weekly using a demountable mechanical gauge at a gauge length of 100 mm. The loading rig was used to adjust the crack widths (via the nuts at the beam ends) as required. The samples were monitored weekly for corrosion potential and rate, and concrete resistivity. The measurement techniques used were similar to those used in Scott's experimental set-up presented earlier.

Two reloading actions were carried out in the 0.4 mm, 0.7 mm and incipient-cracked specimens. The first reloading (between weeks 9 and 10) was done to assess the influence of crack re-opening on the early corrosion rate (up to week 9) while the second reloading (between weeks 18 and 19) was done when corrosion rates had become reasonably stable, to

evaluate whether crack re-opening may increase corrosion rate. Reloading was done by tightening the nuts in the loading rig (Figure 31) to open the 0.4 mm, 0.7 mm and incipient cracks to 0.6 mm, 1.0 mm and 0.2 mm respectively; extra loading rigs were made for reloading the incipient-cracked specimens. The reloading crack widths were selected based on the maximum crack width to which the 0.7 mm crack could be opened without yielding of the steel, i.e. 1.0 mm. The crack widths at reloading were maintained for about 24 hours before being relaxed to their original respective widths.

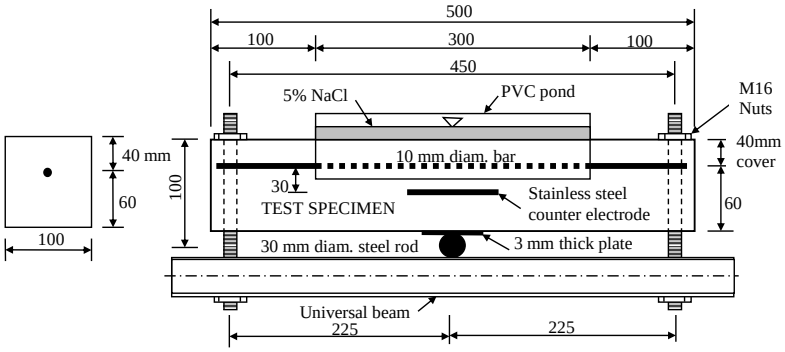

Figure 31: Experimental beam loading set-up and cross section (All dimensions in mm, not to scale)

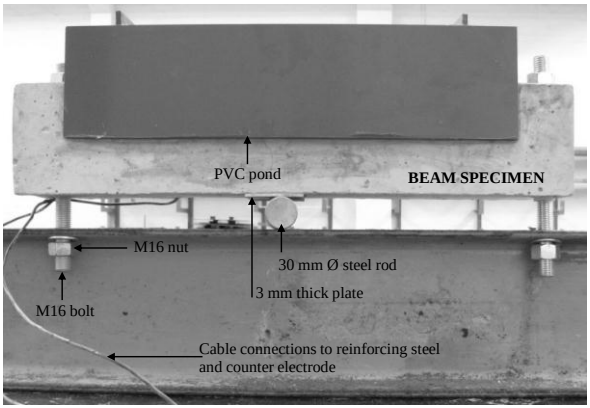

Figure 32: Photograph of a cracked beam rig set-up

MONOGRAPHS IN THIS SERIES

1

Mackechnie, J.R.
Predictions of reinforced concrete durability in the marine environment (1997; revised 2001)

2

Alexander, M.G., Mackechnie, J.R. and Ballim, Y.
Guide to the use of durability indexes for achieving durability in concrete structures (1999)

3

Alexander, M.G., Streicher, P.E. and Mackechnie, J.R.
Rapid chloride conductivity testing of concrete (1999)

4

Alexander, M.G., Ballim, Y. and Mackechnie, J.R.
Concrete durability index testing manual (1999)

5

Mackechnie, J.R. and Alexander, M.G.
Repair principles for corrosion-damaged reinforced concrete structures (2001)

6

Alexander, M.G., Mackechnie, J.R. and Jaufeerally, H.
Structural and durability properties of concrete made with Corex slag (2003)

7

Mackechnie, J.R., Alexander, M.G., Heiyantuduwa, R. and Rylands, T.
The effectiveness of organic corrosion inhibitors for reinforced concrete (2004)

8

Ballim, Y. and Graham, P.C.
A numerical model for predicting early age time-temperature profiles in large concrete structures (2005)

This research was conducted
under the auspices of the

INDUSTRY/NRF PROGRAMME
ON CONCRETE MATERIALS
(with an emphasis on achieving durable
and economical construction under
South African conditions)

Collaborative research by the Universities
of Cape Town and the Witwatersrand